Journal of Virology

Host-Microbial Interactions | Full-Length Text

Transcriptional regulation of the HIV-1 inhibitory factor human mannose receptor 1 by the myeloid-specific transcription factor PU.1

Rosa Mallorson,[1] Eri Miyagi,[1] Sandra Kao,[1] Sayaka Sukegawa,[2] Hideki Saito,[1] Helena Fabryova,[1] Luciana Morellatto Ruggieri,[1] Sonia Mediouni,[3] Susana T. Valente,[3] Klaus Strebel[1]

AUTHOR AFFILIATIONS See affiliation list on p. 21.

ABSTRACT HIV-1 infection of human macrophages leads to the downmodulation of human mannose receptor 1 (hMRC1), a cell-surface glycoprotein that is involved in the host innate immune response. We previously reported that downmodulation of hMRC1 involves the transactivator of transcription (Tat)-dependent transcriptional silencing of the hMRC1 promoter. However, the inhibitory effect of Tat on hMRC1 transcription was indirect and involved inhibition of the transcriptional activator PU.1, which normally upregulates hMRC1 expression in macrophages and other myeloid cells. We cloned a 284-bp fragment of the hMRC1 promoter, and within it, we identified four PU.1 box elements. We assessed the relative contribution of each of the four PU.1 boxes to PU.1-dependent transcriptional regulation and, surprisingly, found that only one of the four PU.1 boxes [PU.1(b)] was critically required for PU.1-mediated upregulation of luciferase expression. Transfer of this PU.1 box to a heterologous promoter conferred PU.1 responsiveness to an otherwise PU.1 insensitive promoter. Electrophoretic mobility shift assays identified this PU.1 box as a direct binding site for PU.1 both in the context of the hMRC1 promoter and the heterologous promoter. Furthermore, mutational analysis of the PU.1 protein identified the C-terminal DNA-binding domain in PU.1 as the region responsible for interaction with the PU.1 box. Recombinant HIV-1 Tat protein did not bind to the hMRC1 promoter element but efficiently interfered with the binding of PU.1 protein to the hMRC1 promoter. Thus, Tat is likely to inhibit the formation of active PU.1 transcription complexes, presumably by binding to and depleting common transcriptional cofactors.

IMPORTANCE HIV-1 infection of cells results in the modulation of cellular gene expression by virus-encoded proteins in a manner that benefits the virus. We reported that HIV-1 transactivator of transcription (Tat) dysregulates the expression of the human mannose receptor 1 (hMRC1). hMRC1 is involved in the innate immune response of macrophages to foreign pathogens. Tat does not act directly on the hMRC1 promoter but instead inhibits PU.1, a cellular transcription factor regulating hMRC1 gene expression. Here, we characterize the PU.1-dependent regulation of hMRC1 expression. We identified four potential PU.1 binding sites in the hMRC1 promoter region but found that only one, PU.1(b), functioned as a true binding site for PU.1. Transfer of the PU.1(b) box to a heterologous promoter did not activate this promoter *per se* but rendered it responsive to PU.1. Our results support the view that PU.1 acts as a transcriptional co-factor whose activity can be regulated by HIV-1 Tat.

KEYWORDS HIV-1, Tat, mannose receptor promoter , PU.1, transcription factor , transcriptional regulator

Editor Frank Kirchhoff, Ulm University Medical Center, Ulm, Germany

Address correspondence to Klaus Strebel, kstrebel@nih.gov.

Rosa Mallorson and Eri Miyagi contributed equally to this article. Author order was determined alphabetically.

The authors declare no conflict of interest.

See the funding table on p. 21.

Received 1 November 2023
Accepted 17 November 2023
Published 11 December 2023

We previously reported that the cell surface receptor human mannose receptor C-type 1 (hMRC1) can inhibit virus particle release from infected macrophages via a mechanism that phenotypically resembles the inhibition of virus detachment from BST-2 expressing HIV-1-infected cells (1). Interestingly, hMRC1 aids HIV-1 binding to monocyte-derived macrophages (MDM) and endocytic uptake of the virus (2). While mechanistic details of the BST-2 mediated inhibition of virus release remain unclear, it is well-accepted that the antiviral effect of BST-2 can be neutralized by defined virus-encoded proteins, e.g., Vpu in the case of HIV-1, Env in the case of HIV-2, and Nef in the case of some SIV isolates [for review see reference (3)]. Thus, viral accessory proteins have the capacity to modulate the expression and/or function of host restriction factors. There is less of a consensus concerning the regulation of hMRC1 expression in HIV-1-infected macrophages. While there is agreement that HIV-1 infection of macrophages results in both downmodulation of hMRC1 from the cell surface as well as a reduction of total cellular protein levels, there is an ongoing debate on how HIV-1 accomplishes this task. While several reports implicate Tat (transactivator of transcription) (1, 2, 4), others did not find a significant contribution of Tat to the downmodulation of hMRC1 (5). The contribution of Nef to the downmodulation of hMRC1 from the cell surface is undisputed; however, Nef does not appear to affect the total cellular steady-state levels of hMRC1 (5, 6). Finally, one recent study identified the role of Vpr in the downmodulation of hMRC1 at the total cellular protein level (5). The authors report that the expression of Vpr reduces hMRC1 steady-state levels through a mechanism that requires interaction with DCAF1 but does not involve degradation of hMRC1 by the proteasomal pathway normally used by Vpr to degrade other substrates such as UNG2 (5). Our own investigation of HIV-1-infected macrophages did not reveal a significant contribution of any of the viral accessory proteins. Indeed, the inactivation of *vif*, *vpu*, *nef*, or *vpr* genes alone when studied in the context of the macrophage-tropic full-length infectious HIV-1 AD8 molecular clone did not abolish its ability to inhibit hMRC1 expression at the total protein level (2). Thus, if viral accessory proteins are involved in downmodulating hMRC1 at the protein level, it would have to be through a concerted effort of more than one accessory protein.

Instead, our own experiments suggest that HIV-1-induced downmodulation of hMRC1 occurs primarily at the transcriptional level (1, 2) and involves the activity of HIV-1 Tat. Tat is a transcriptional regulator that activates transcription from the HIV-1 LTR promoter but has been associated with additional functions as well (7–11). Indeed, a genome-wide screen identified about 500 direct Tat binding sites in the human genome. About half of these targets were upregulated by Tat, while the other half was inhibited (12). Thus, the inhibitory effect of Tat on the expression of hMRC1 reported in our previous study (2) is not unique and compatible with the reported genome-wide effects. Interestingly, we found that the effect of Tat on the inhibition of hMRC1 expression was not direct but mediated by the inhibition of another transcription factor, PU.1 [also referred to as SPI-1 proto-oncogene (13)]. Aside from the *hMRC1* gene, PU.1 regulates the expression of more than 100 additional cellular genes, affecting the developmental landscape via combinatorial control with other regulators (14–18). Our previous experiments demonstrated that PU.1 is critical not only for the transcriptional regulation of hMRC1 in primary macrophages but is also required in HEK293T cells, which do not express PU.1 endogenously (2). Indeed, the expression of luciferase from an hMRC1 promoter-driven indicator vector in HEK293T cells was almost undetectable when analyzed alone but could be activated in a dose-dependent manner by co-expression of PU.1 in *trans* (2).

Our current study aimed at a more detailed characterization of the transcriptional regulation of the hMRC1 promoter by PU.1. PU.1 recognizes a 5-bp core sequence 5′-TTCCT-3′ (referred to as PU.1 box) or its reverse complement 5′-AGGAA-3′ (19–22). We found that a 284-bp hMRC1 promoter fragment contained four PU.1 boxes. Interestingly, only one of the four PU.1 boxes referred to as PU.1(b) was critical for PU.1 responsiveness, and mutation or deletion of this element led to a dramatic reduction in PU.1 response.

Electrophoretic mobility shift assays (EMSA) identified PU.1(b) as a direct binding site for PU.1 and the transfer of the PU.1(b) box to a heterologous promoter conferred PU.1 recognition. Moreover, mutational analysis of PU.1 protein revealed a critical role for its C-terminal DNA-binding domain for the regulation of the hMRC1 promoter.

Finally, using recombinant Tat protein, we were able to demonstrate the interference of Tat with the binding of PU.1 protein to the hMRC1 promoter. This was not due to competitive binding of PU.1 and Tat to the hMRC1 promoter since Tat alone did not bind the hMRC1 promoter. Taken together, our data provide new insights into the transcriptional regulation of hMRC1 by the myeloid cell-specific transcription factor PU.1.

RESULTS

The hMRC1 promoter contains four potential PU.1 binding sites

We previously reported that the transfer of a 150-bp sequence element from upstream of the transcriptional start site for the hMRC1 gene (*hMRC1*) into a luciferase indicator plasmid was sufficient to render it responsive to the myeloid-specific transcription factor PU.1 (2). The promoter element had very low basal activity in the absence of PU.1. The 150-bp hMRC1 promoter element contains three sequence elements previously defined as PU.1 boxes (20). They are denoted as PU.1(a), PU.1(b), and PU.1(c), respectively, in Fig. 1. Interestingly, analysis of the rat mannose receptor promoter region also revealed the presence of three PU.1 boxes within a 170-bp region upstream of the transcription start site (19). Inspection of the GenBank sequence for the *hMRC1* gene revealed a fourth PU.1 box approximately 220 bp upstream of the transcription start site [denoted PU.1(d) in Fig. 1].

To analyze the importance of these PU.1 boxes for PU.1 responsiveness, we cloned a 284-bp fragment of the human mannose receptor promoter into the promoter trap vector pGL3-luc (Promega, Madison, WI, USA) resulting in pGL284 and used it as basis

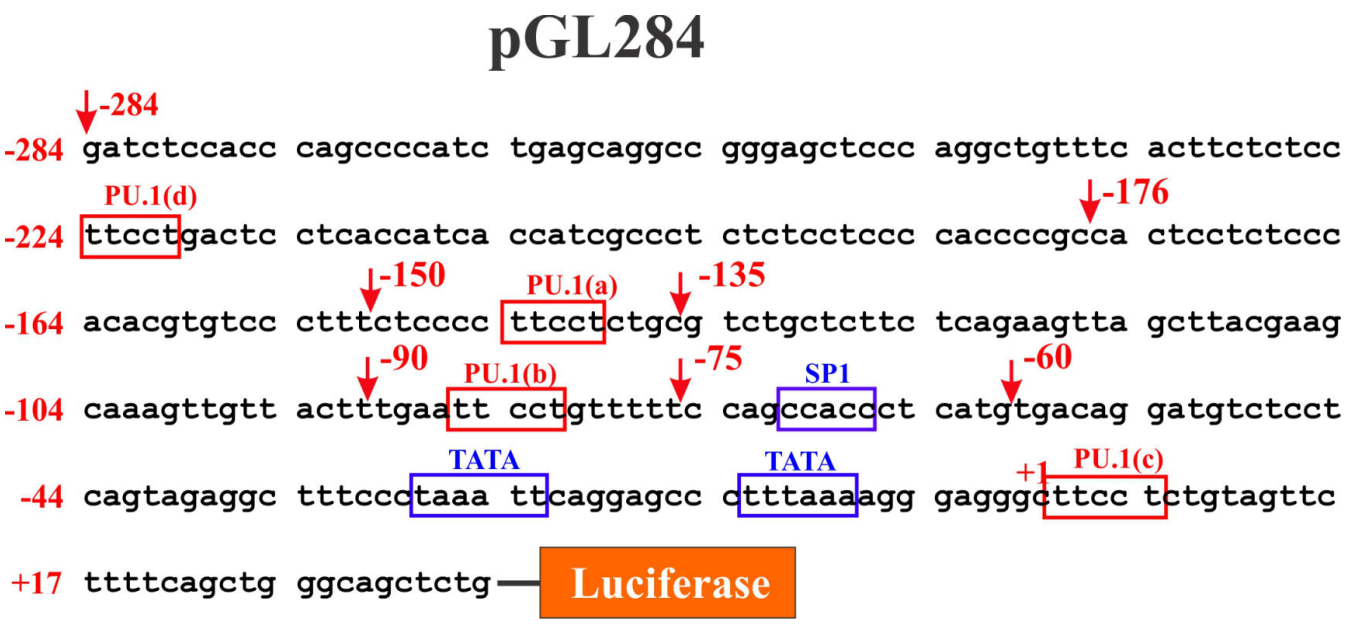

FIG 1 Cloning of the hMRC1 promoter. Based on the hMRC1 promoter sequence reported by Rouleux et al. (23) and cross comparison with GenBank entry NG_047011.1 (positions 4,703–5,021), a 342-bp gBlock DNA fragment was synthesized (IDT, Coralville, IA, USA). The gBlock fragment encompassed residues −284 to +36 of the hMRC1 gene (position 1 being defined as transcription start site), as well as upstream HindIII and downstream NcoI restriction sites (not shown) for cloning into the promoter trap vector pGL3-basic (Promega, Madison, WI, USA). This resulted in plasmid pGL284. Promoter activity in pGL284 is measured as activation of the downstream luciferase gene, which can be quantified in a standard luciferase assay. Blue boxes represent TATA-box and SP1 transcriptional elements, respectively. Red boxes indicate putative PU.1 binding sites [PU.1(a), PU.1(b), PU.1(c), and PU.1(d)]. Positions of 5′ deletions created in Fig. 2 are marked by red arrows.

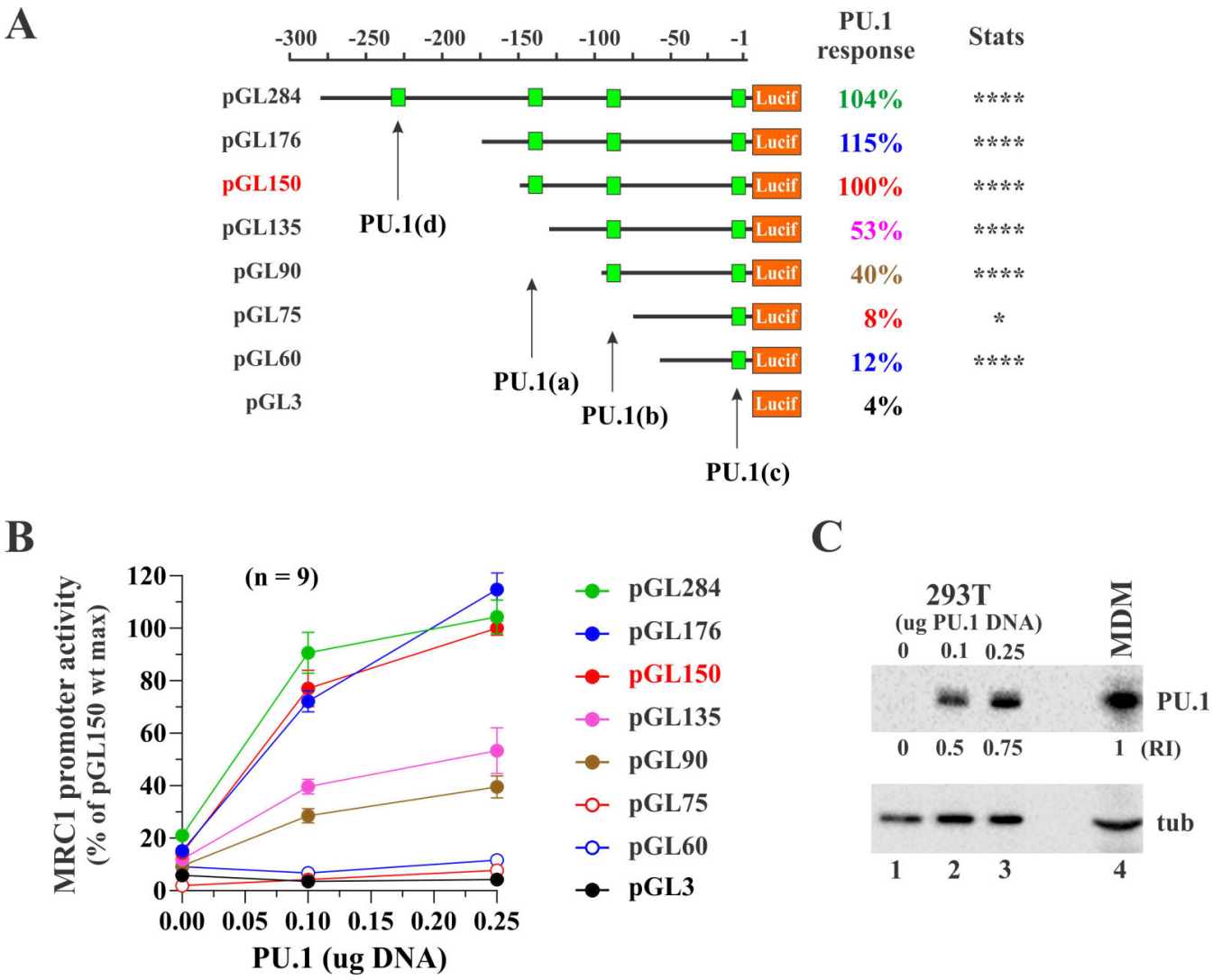

FIG 2 The PU.1 binding motifs are required for responsiveness to PU.1. (A) Schematic representation of the deletion mutants used. Deletions of increasing length were introduced into pGL284 via oligonucleotide-based mutagenesis using the oligonucleotides listed in Table 1. The putative PU.1 binding sites are indicated as green boxes. (B) Constant amounts of the listed indicator plasmids (0.20 µg each) were cotransfected with increasing amounts (0, 0.1, and 0.25 µg) of pcDNA-PU.1 expression vector. All samples were transfected into HEK293T cells in 24-well plates. Amounts of transfected DNAs were adjusted to 0.45 µg per well using empty vector DNA as needed. Each experiment was done three times in triplicate (total $n = 9$). After 24 h, cells were lysed in 1× reporter lysis buffer (Promega, Madison, WI, USA), and luciferase activity in each sample was quantified as described in Materials and Methods. Results were plotted as a function of PU.1 concentration. The signals obtained with pGL150 at the highest concentration of PU.1 (0.25 µg) were empirically defined as 100%, and signals obtained with the other constructs were expressed relative to pGL150. Error bars show the standard error of the mean, calculated from nine replicate samples. PU.1 response is expressed as the relative mean luciferase activity for each construct at 0.25 µg PU.1 DNA (panel A, right). Statistical significance of the differences of individual constructs relative to the empty vector (pGL3) was determined for the highest concentration of PU.1 (0.25 µg) using an unpaired two-tailed *t*-test (GraphPad Prism). Results are integrated into panel A (Stats). ****$P < 0.0001$ and *$P < 0.05$. (C) Comparison of levels of endogenously and exogenously expressed PU.1. HEK293T cells were transfected in a 24-well plate with 0.1 µg (lane 2) or 0.25 µg (lane 3) of untagged PU.1 vector. A mock-transfected sample was included as negative control (lane 1). Whole-cell extract from uninfected MDM cells was used as a reference for endogenous expression of PU.1. Sample loading was adjusted to achieve comparable signals for tubulin (tub, lane 4). Two sets of samples were run side-by-side on the same gel. One set was probed with PU.1 specific antibodies (top panel); the other one was probed with antibodies to tubulin (lower panel). PU.1 and tubulin signals were quantified using Multi Gauge software (FujiFilm). PU.1 signals were corrected for fluctuations in tubulin levels and expressed as relative intensity (RI) with the signal from the macrophage extract being defined as 1.

for the creation of other promoter variants. To start, we created a series of 5′ truncations by deleting increasing portions of the hMRC1 promoter from within pGL284 (Fig. 2A).

TABLE 1 Oligonucleotide primers and templates for site-directed mutagenesis and cloning

Primer designation	Primer sequence
hMRC1 promoter 5′ truncations (Fig. 2)	
pGL 176F	5′ CTGCGATCTAAGTAAGCTTG CACTCCTCTCCCACAC
pGL 176R	5′ GTGTGGGAGAGGAGTGCAAGCTTACTTAGATCGCAG
Template: pGL284	
pGL 150F	5′ CTGCGATCTAAGTAAGCTTG TCTCCCCTTCCTCTGCGTCT
pGL 150R	5′ AGACGCAGAGGAAGGGGAGACAAGCTTACTTAGATCGCAG
Template: pGL284	
pGL 135F	5′ CTGCGATCTAAGTAAGCTTG GTCTGCTCTTCTCAGAAGTT
pGL 135R	5′ AACTTCTGAGAAGAGCAGACCAAGCTTACTTAGATCGCAG
Template: pGL284	
pGL 90F	5′ CTGCGATCTAAGTAAGCTTG TGAATTCCTGTTTTTCCAGC
pGL 90R	5′ GCTGGAAAAACAGGAATTCACAAGCTTACTTAGATCGCAG
Template: pGL284	
pGL 75F	5′ CTGCGATCTAAGTAAGCTTG CCAGCCACCCTCATGTGACA
pGL 75R	5′ TGTCACATGAGGGTGGCTGGCAAGCTTACTTAGATCGCAG
Template: pGL284	
pGL 60F	5′ CTGCGATCTAAGTAAGCTTG TGACAGGATGTCTCCTCAGT
pGL 60R	5′ ACTGAGGAGACATCCTGTCACAAGCTTACTTAGATCGCAG
Template: pGL284	
Internal deletions in the hMRC1 promoter (Fig. 3A)	
D30-5F	5′- CTCAGTAGAGGCTTTCGGAGGGCTTCCTCTGT
D30-5R	5′- ACAGAGGAAGCCCTCCGAAAGCCTCTACTGAG
Template: pGL150	
D60-30F	5′ TCCAGCCACCCTCATGC CTAAATTCAGGAGCC
D60-30R	5′ GGCTCCTGAATTTAGGCATGAGGGTGGCTGGA
Template: pGL150	
D75-30-5	5′ TTTGAATTCCTGTTTT TCCTAAATTCAGGAGCC
D75-30-3	5′ GGCTCCTGAATTTAGGAAAAACAGGAATTCAAA
Template: pGL150	
D135-90-5	5′ TCTCCCCTTCCTCTGCTGAATTCCTGTTTTTC
D135-90-3	5′ GAAAAACAGGAATTCAGCAGAGGAAGGGGAGA
Template: pGL150	
PU.1 box mutations and deletions in the hMRC1 promoter (Fig. 3B)	
150-Del(a)F	5′ CTGCGATCTAAGTAAGCTTGTCTCCCCCTGCGTCTGCTCT
150-Del(a)R	5′ AGAGCAGACGCAGGGGGAGACAAGCTTACTTAGATCGCAG
Template: pGL150	
150-Del(b)F	5′ AAGTTGTTACTTTGAAGTTTTTCCAGCCACCC
150-Del(b)R	5′ GGGTGGCTGGAAAAACTTCAAAGTAACAACTT
Template: pGL150	
150-mut(a)F	5′ GTAAGCTTGTCTCCCCAGAAGCTGCGTCTGCTCTTCT
150-mut(a)R	5′ AGAAGAGCAGACGCAGCTTCTGGGGAGACAAGCTTAC
Template: pGL150	
150-mut(b)F	5′ CAAAGTTGTTACTTTGAAAGAAGGTTTTTCCAGCCACCCTC
150-mut(b)R	5′ GAGGGTGGCTGGAAAAACCTTCTTTCAAAGTAACAACTTTG
Template: pGL150	
150-mut(ab)F	5′ ACGTGTCCCTTTCTCCCCAGAAGCTGCGTCTGCTCTTCTCA
150-mut(ab)F	5′ TGAGAAGAGCAGACGCAGCTTCTGGGGAGAAAGGGACACGT
Template: pGL150mut(b)	
150-del(ab)F	5′ GTAAGCTTGTCTCCCCCTGCGTCTGCTCTTCT
150-del(ab)F	5′ AGAAGAGCAGACGCAGGGGGAGACAAGCTTAC
Template: pGL150del(b)	

(*Continued on next page*)

TABLE 1 Oligonucleotide primers and templates for site-directed mutagenesis and cloning (*Continued*)

Primer designation	Primer sequence
Transfer of PU1(b) element into pGL-3xNFkB (Fig. 5)	
PU.1(b1)F	5′-GCGTGCTAGCCCGGGCTCGAGATTGAATTCCTGTTTTTCTGCGATCTAAGTAAGCTTGC
PU.1(b1)R	5′ GCAAGCTTACTTAGATCGCAGAAAAACAGGAATTCAATCTCGAGCCCGGGCTAGCACGC
PU.1(b2)F	5′ TCTAAGTAAGCTTGCATGCCTGTTGAATTCCTGTTTTCAGTCGACATGTGGGACTTTCC
PU.1(b2)R	5′ GGAAAGTCCCACATGTCGACTGAAAACAGGAATTCAACAGGCATGCAAGCTTACTTAGA
Construction of pcDNA-PU.1-HA[a]	
5′ primer	5′ TCTAGA**CTCGAG**CGGCCCACCATGGAAGGG
3′ primer	5′ TTATT**GGATC C**TACGCGTAA TCTGGGACGT CGTAAGGGTA GTGGGGCGGGTGGCGCCGCT CGG
Primers for hMRC1 EMSA probes (Fig. 4)	
EMSA-1F	5′ CTCGAGATCTGCGATCTAAG
EMSA-1R	5′ TCTTCCAGCGGATAGAATGG
Primers for NFkB EMSA probes (Fig. 5)	
EMSA-2F	5′ TACGCGTGCTAGCCCGGGC
EMSA-2R	5′ ACTCTAATGCGCGCGGACCG
PU.1 N-terminal deletions [PU.1 (97–264) and PU.1 (151–264)] (Fig. 6)	
PU.1 97–264F	5′ GACTCGAGCGGCCCACCATGACCCCCATGGTGCCACCCCA
PU.1 97–264R	5′ TGGGGTGGCACCATGGGGGTCATGGTGGGCCGCTCGAGTC
PU.1 151–264F	5′ GACTCGAGCGGCCCACCATGGGCCTGGAGCCCGGGCCTGG
PU.1 151–264R	5′ CCAGGCCCGGGCTCCAGGCCCATGGTGGGCCGCTCGAGTC
PU.1 C-terminal deletion [PU.1 (1–150)] (Fig. 6)	
PU.1 1–150F	5′ GGAGGTGTCTGACGGCGAGGCGGATTACCCTTACGACGTCCCAGATTACG
PU.1 1–150R	5′ CGTAATCTGGGACGTCGTAAGGGTAATCCGCCTCGCCGTCAGACACCTCC

[a]The XhoI and BamHI sites used for cloning are underlined and shown in bold; the PU.1 translation start site in the 5′ primer is underlined; the HA epitope (YPYDVPDYA) is encoded in the 3′ primer.

The resulting mutants were cotransfected with increasing amounts of wild-type PU.1 expression vector. Activation of luciferase expression was monitored by a standard luciferase assay (Fig. 2B). Since our previous study employed pGL150, we decided to use this vector as our reference and defined maximal activation by PU.1 from pGL150 as 100%. We found that deletion of the upstream PU.1 box [PU.1(d)], as was done in pGL176 or pGL150, did not impact the response to PU.1 (pGL284: 104%; pGL176: 115%). In contrast, deletion of PU.1(a) in pGL135 and pGL90 essentially cut the PU.1 response in half (pGL135: 53%; pGL90: 40%). Further deletions in the hMRC1 promoter that additionally eliminated PU.1(b) reduced PU.1 response to near background levels [compare empty vector pGL3 (4%) to pGL75 (8%) and pGL60 (12%)]. In all cases, the PU.1(c) element remained intact, suggesting that the PU.1(c) element did not significantly contribute to PU.1-regulated gene expression. Since PU.1(c) overlaps the transcription start site, we did not further analyze this element. We should note that the levels of exogenously expressed PU.1 employed in our experiments are comparable to the endogenous PU.1 levels observed in uninfected primary human macrophages (Fig. 2C). We conclude that the region in the hMRC1 promoter containing PU.1(a) and PU.1(b) boxes is critical for PU.1 responsiveness, whereas sequences upstream of PU.1(a), including PU.1(d), did not contribute significantly to PU.1 responsiveness.

Deletion or mutation of PU.1(a) and PU.1(b) boxes in the hMRC1 promoter eliminates PU.1 responsiveness

Our next goal was to identify the region on the hMRC1 promoter responsible for PU.1 response. For that purpose, we constructed an additional set of promoter mutants using pGL150 as our basis vector (Fig. 3). First, we deleted the sequences outside the PU.1 boxes that included intervening sequences between PU.1(a) and PU.1(b) (Fig. 3A, pGLΔ135–90), as well as sequences between PU.1(b) and the transcription start site (pGLΔ30–5, pGLΔ60–30, and pGLΔ75–30). Interestingly, deletion of intervening sequences between PU.1(a) and PU.1(b) (pGLΔ135–90) only modestly affected PU.1

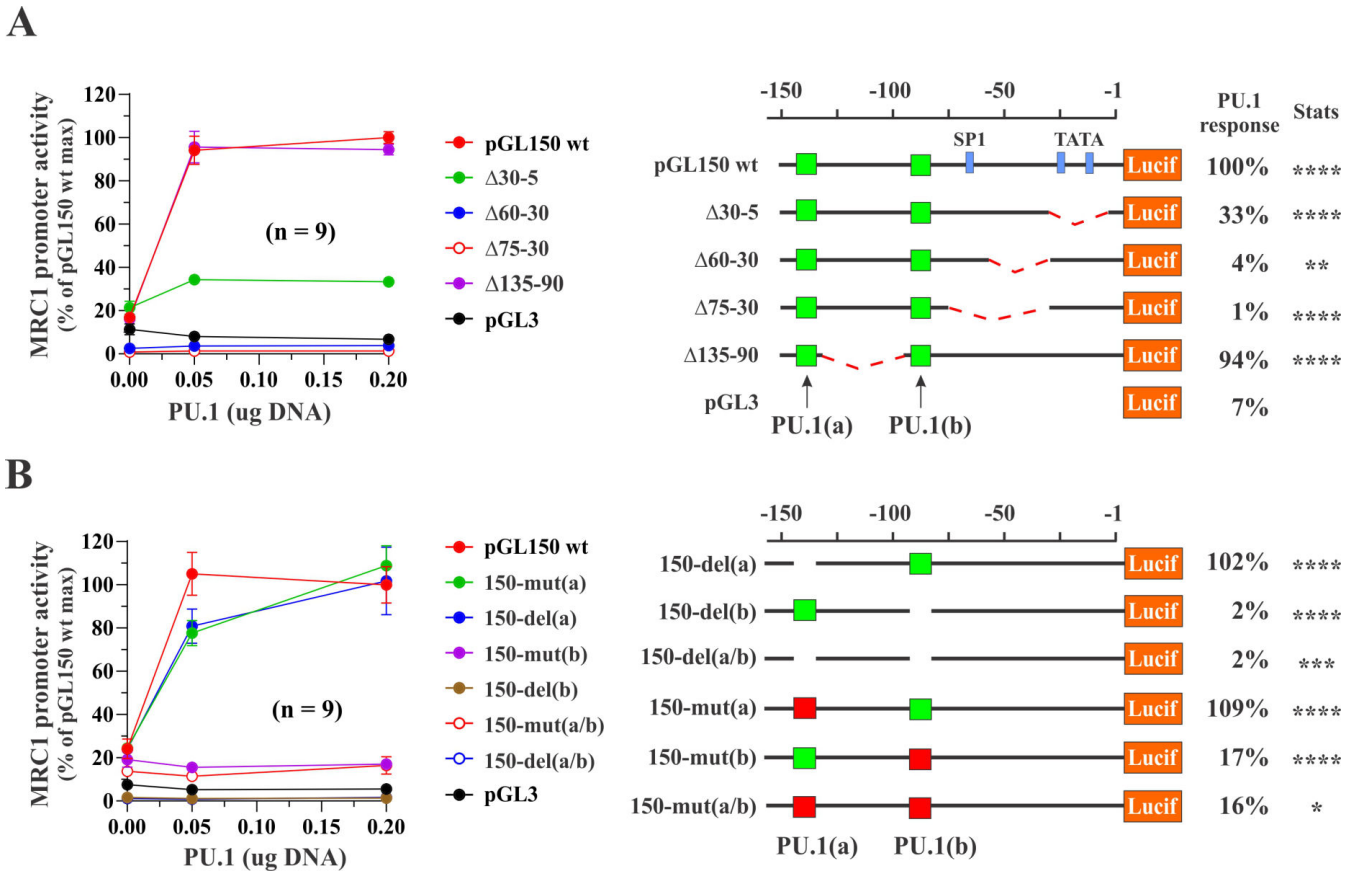

FIG 3 Mutational analysis of the hMRC1 promoter fragment in pGL150. (A) Deletion of sequences outside the potential PU.1 binding motifs in the backbone of pGL150 was accomplished by oligonucleotide-directed mutagenesis as described in Materials and Methods using the primers listed in Table 1. Constant amounts (0.2 µg) of the resulting indicator plasmid DNAs were cotransfected into HEK293T cells together with increasing amounts of pcDNA-PU.1 expression vector (0, 0.05, and 0.2 µg). Transfections were performed in 24-well plates three times independently in triplicate (n = 9). Total amounts of transfected DNA per well were adjusted to 0.4 µg using empty vector DNA as needed. Results were plotted as a function of PU.1 concentration. Error bars show the standard error of the mean calculated from nine replicates. The signals obtained with pGL150 wt at the highest concentration of PU.1 (0.2 µg) were defined as 100%, and signals obtained with the other constructs were expressed relative to pGL150. PU.1 responses (numbers on the right) are expressed as the relative mean luciferase activity for each construct at 0.2 µg PU.1 DNA. (B) Deletion or mutation of the putative PU.1 binding sites results in loss of PU.1 responsiveness. PU.1 binding motifs (TTCCT; see Fig. 1) in pGL150 were either deleted (5-bp deletion) or mutated (TTCCT to AGAAG) as indicated in the cartoon by oligonucleotide-based mutagenesis using the primer pairs listed in Table 1. Wild-type PU.1 boxes are indicated in green. Mutated PU.1 boxes are indicated in red. Deletions are represented as gaps. Resulting plasmid DNAs (0.2 µg each) were cotransfected into HEK293T cells with increasing amounts (0, 0.05, and 0.2 µg) of pcDNA-PU.1 expression vector. Total amounts of transfected DNA per well were adjusted to 0.4 µg using empty vector DNA as needed. Samples were processed and promoter activation was quantified as in panel A. Error bars show the standard error of the mean calculated from nine technical replicates. PU.1 responses (numbers on the right) are expressed as the relative mean luciferase activity for each construct in the presence of 0.2 µg PU.1 vector DNA. Statistical significance of the differences of individual constructs relative to the empty vector (pGL3) was determined for the highest concentration of PU.1 (0.20 µg) using an unpaired two-tailed t-test (GraphPad Prism). Results are integrated into the graphical display on the right (Stats). ****P < 0.0001; ***P < 0.001; **P < 0.01; and *P < 0.05.

response (94%). In contrast, deletion of sequences between the transcription start site and PU.1(b) (pGLΔ30–5, pGLΔ60–30, and pGLΔ75–30) significantly impaired PU.1 dependent transcriptional activation of the luciferase gene. The latter observation is not surprising since the region affected by the deletions contains other transcriptional regulatory elements, including two TATA boxes and one SP1 binding site that may be required for transcriptional activation.

To further assess the importance of the PU.1 boxes for PU.1-induced activation of the hMRC1 promoter, we created a series of mutants that involved deletion or mutation of one or both of the PU.1(a) and PU.1(b) boxes (Fig. 3B). Deletion of the PU.1 boxes was accomplished by deleting the TTCCT core sequences of the PU.1 boxes (Fig. 3B, gaps).

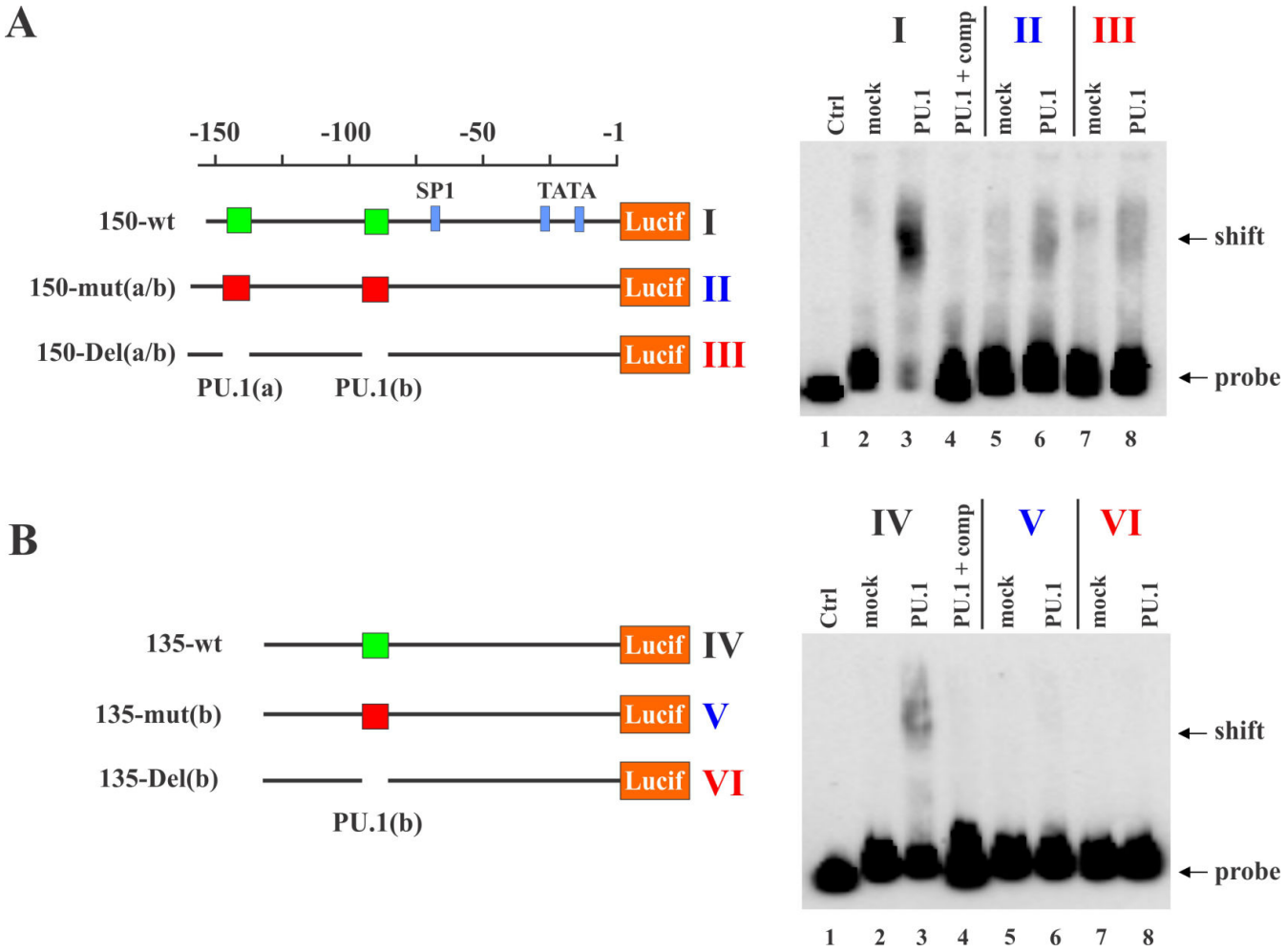

FIG 4 The TTCCT motifs in the hMRC1 promoter represent binding sites for PU.1. (A) Templates used for the gel shift analysis are shown as cartoons on the left. EMSA of pGL150 wt or mutants. A 272-bp fragment encompassing hMRC1 promoter region −150 to +36 (see Fig. 1) was PCR amplified using primers EMSA-1F and EMSA-1R and pGL150-based templates. Biotinylated probes of hMRC1 promoter sequences from either wild-type (150-wt), mutated [150-mut(a/b)], or PU.1 site deleted [150-del(a/b)] constructs were created as described in Materials and Methods. (B) EMSA of pGL135-based promoter variants. The experiment is like panel A, except that the distal PU.1(a) binding motif is missing (see Fig. 1). The resulting EMSA probe was 257-bp long. (A and B) Biotinylated probes were incubated with nuclear extracts from mock-transfected HEK293T cells (lanes 2, 5, and 7) or from cells expressing PU.1 (lanes 3, 4, 6, and 8). A non-biotinylated competitor probe (comp) was included with the wt biotinylated probes as specificity control (lane 4). Finally, biotinylated probes alone were included as an additional control (lane 1). After incubation of probes and cell extracts, samples were subjected to electrophoresis on 4.5% non-denaturing acrylamide gel. Samples were then transferred to positively charged nylon membranes and probed with a streptavidin-HRP conjugate (LightShift Chemiluminescent EMSA Kit, Thermo Scientific, Waltham, MA, USA). Images were acquired on a BioRad ChemiDoc MP system and processed using ImageLab 6.0 software. Roman numerals (I–VI) connect the EMSA data to the corresponding graphical display of the respective probes.

Mutation of the PU.1 boxes was accomplished by replacing the TTCCT core sequence with AGAAG (Fig. 3B, red boxes). We found that deletion or mutation of the PU.1(a) box did not affect the response to PU.1 [150-del(a): 102% and 150-mut(a): 109%, respectively]. In contrast, deletion or mutation of PU.1(b) alone or in combination with PU.1(a) dramatically reduced PU.1-mediated activation of the hMRC1 promoter. These results suggest that the PU.1(b) box element is critically important for PU.1 responsiveness, while in the context of pGL150, the PU.1(a) box played only a secondary role.

PU.1(b) is a binding site for the PU.1 transcription factor

To demonstrate that PU.1(b) constitutes a direct binding site for PU.1 protein, we performed EMSA, which can measure protein-DNA interactions. For that purpose,

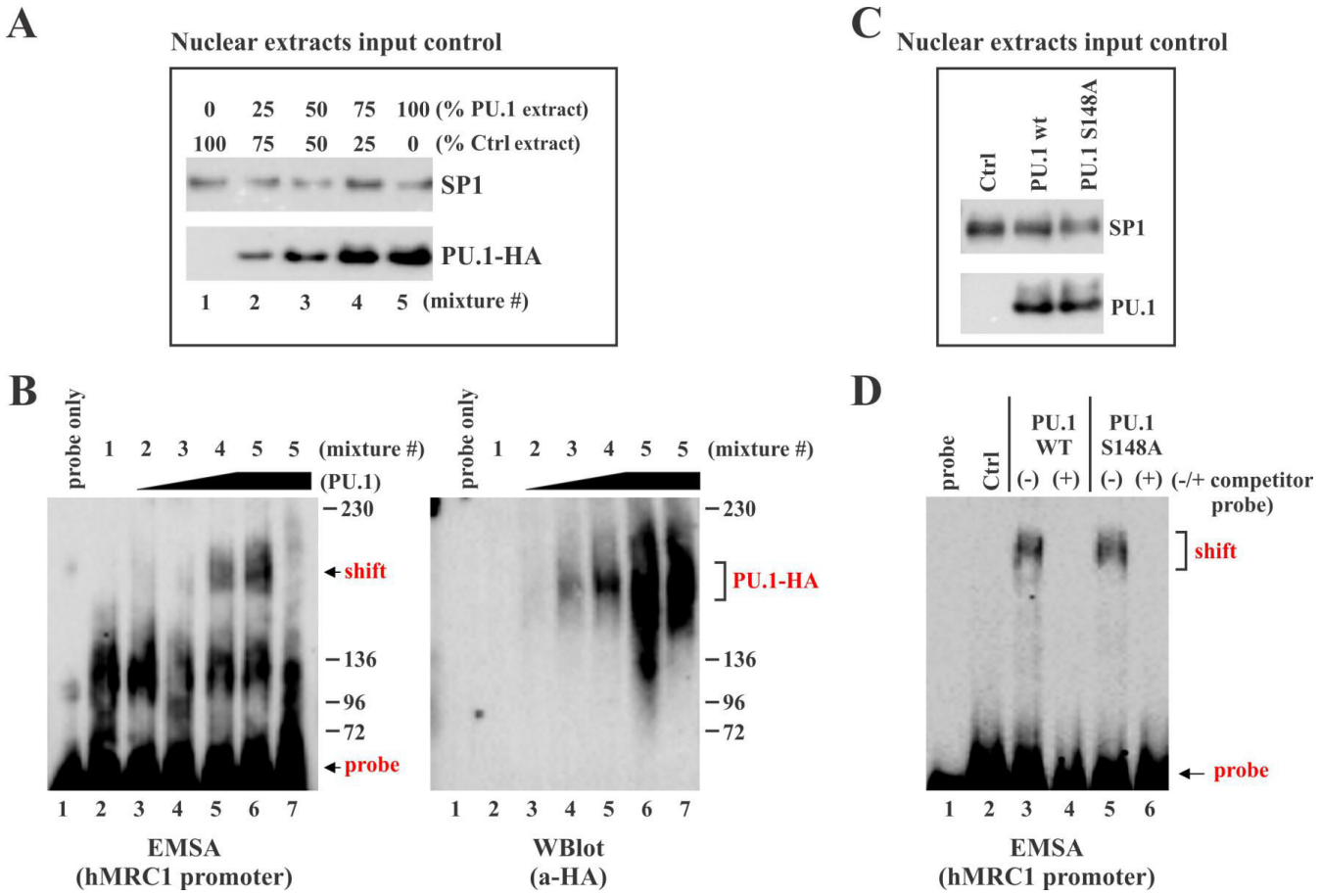

FIG 5 (A and B) The PU.1-induced change in the electrophoretic mobility of the hMRC1 probe is dose dependent. (A) For the production of nuclear extracts, HEK293T cells were either mock transfected with 7 µg of empty vector [pcDNA3.1(-)] or transfected with 7 µg of pcDNA-PU.1-HA. Transfected cells were harvested 24 h later, and nuclear extracts were prepared as described in Materials and Methods. Nuclear extracts were mixed in various ratios [100% mock extract (lane 1); 25% PU.1-HA extract (lane 2); 50% PU.1-HA extract (lane 3); 75% PU.1-HA extract (lane 4); and 100% PU.1 (lane 5)]. PU.1-HA levels in the various mixtures were verified by immunoblotting using an antibody to the HA epitope in PU.1-HA. As a control for equal amounts of nuclear extract, samples were also probed with an antibody to the endogenous nuclear transcription factor SP1. (B) To demonstrate that the electrophoretic mobility shift of the hMRC1 probe is affected by varying levels of PU.1, the biotinylated hMRC1 probe "150-wt" (see Fig. 4A), was incubated with various mixtures of the nuclear extracts described in panel A (extracts #1–5) for 30 min at room temperature. The samples in lane 7 received a 100-fold excess of unlabeled competitor DNA as described in Fig. 4A, lanes 3 and 4. Samples were then split in half and both sets were subjected to electrophoresis on 4.5% non-denaturing acrylamide gels. One set was processed for EMSA as in Fig. 4A (left panel), and the other set was processed for immunoblotting using an antibody to the HA tag in PU.1 (right panel). The positions of the shifted probe on the EMSA blot and the PU.1 protein on the immunoblot, respectively, are indicated in red. (C and D) Mutation of S148 in PU.1 does not impair the ability of PU.1 to bind to the hMRC1 promoter and induce a shift in the electrophoretic mobility of the hMRC1 promoter probe. (C) HEK293T cells were mock transfected with 7 µg of empty vector (Ctrl) or were transfected with 7 µg of pcDNA-PU.1-HA (PU.1 wt) or pcDNA-PU.1 S148A-HA (PU.1 S148A). Transfected cells were harvested 24 h later, and nuclear extracts were prepared as in panel A. Protein expression of PU.1 wt and PU.1 S148A as well as SP1 was assessed by immunoblotting as in panel A. (D) EMSA of PU.1 wt and PU.1 S148A in the absence (–) or presence (+) of unlabeled competitor DNA probe was similarly performed as described in Fig. 4A. Positions of the unshifted and shifted probe are indicated in red.

we created biotinylated probes corresponding to the promoter sequences present in pGL150 (Fig. 4A) or pGL135 (Fig. 4B). Biotinylated probes were made as described in Materials and Methods using wild-type promoter sequences or sequences containing PU.1 box mutations (red boxes) or deletions (gaps) as templates as indicated in the cartoons. The probes were then incubated with nuclear extracts from cells exogenously expressing PU.1. Nuclear extracts from mock-transfected cells were used as control (mock). The specificity of the DNA-protein interaction was demonstrated by the addition of a 100-fold excess of unlabeled competitor DNA (Fig. 4A and B, lane 4). Details of the EMSA procedure are described in Materials and Methods. Briefly, protein-DNA complexes

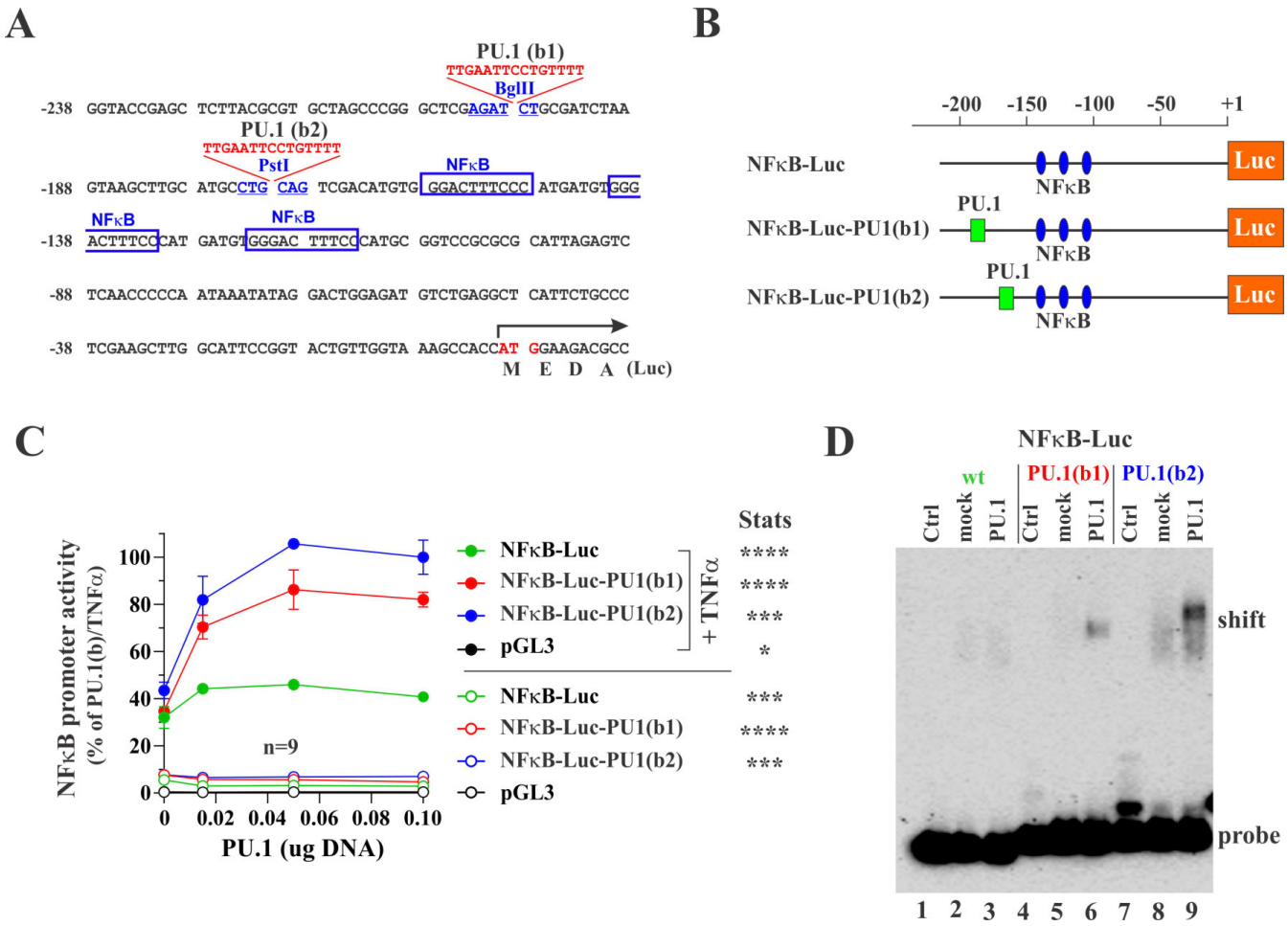

FIG 6 Transfer of the hMRC1 PU.1(b) motif into a heterologous promoter confers PU.1 responsiveness. (A) Nucleotide sequence of the pGL-3xNFκB-Luc promoter region. The vector contains three NFκB sites marked by blue boxes. The translational start site (ATG) for luciferase is shown in red. A 15-bp fragment encompassing the TTCCT recognition sequence together with 5′ and 3′ flanking residues of PU.1(b) (5 bp each; see Fig. 1) was inserted at two different positions [PU.1(b1) and PU.1(b2)] as shown using oligonucleotide-based mutagenesis. Both insertions are upstream of the three NFκB binding sites. The sequences of the oligonucleotides used to create these constructs are listed in Table 1. (B) Schematic presentation of the NFκB-Luc-PU.1 constructs. The three NFκB binding sites are represented by the blue ovals. PU.1(b) boxes are depicted in green. (C) Response of the NFκB-Luc-PU.1(b) promoter constructs to PU.1 was determined by co-transfecting the indicator plasmids (0.15 µg each) together with increasing amounts (0, 0.015, 0.05, and 0.1 µg) of pcDNA-PU.1 plasmid DNA. Total amounts of transfected DNA per well were adjusted to 0.4 µg using empty vector DNA as needed. Luciferase production was measured 30 h after transfection. Eight hours prior to that, cells were either stimulated for 15 min with TNFα (10 ng/mL) (solid circles) or were left untreated (open circles). TNFα-containing medium was then replaced by 1 mL of fresh Dulbecco's modified Eagle's medium (DMEM), and cells were cultured for 8 h. Promoter activity was calculated as a percentage of the signal obtained with the NFkB-Luc-PU.1(b2) construct at the highest level of PU.1 (0.1 µg), which was defined as 100%. All experiments were done three times in triplicate ($n = 9$), and error bars represent the standard error of the mean. Statistical significance of the differences of individual constructs relative to the empty vector (pGL3) was determined for the highest concentration of PU.1 (0.10 µg) using an unpaired two-tailed *t*-test (GraphPad Prism). Results are integrated into the graphical display on the right (Stats). ****$P < 0.0001$; ***$P < 0.001$; and *$P < 0.05$. (D) EMSA reveals the binding of PU.1 to PU.1(b) elements in the backbone of the NFκB-Luc vector. Biotinylated EMSA probes were produced, and samples were processed as described in Materials and Methods using primers EMSA-2F and EMSA-2R (Table 1) and pGL-3xNFκB-Luc as a template. Untreated HEK293T cells (mock) or HEK293T cells transfected with pcDNA-PU.1 wt (PU.1) were stimulated 14 h after transfection for 15 min with TNFα (10 ng/mL). TNFα-containing medium was then removed and replaced with full Dulbecco's modified Eagle's medium (DMEM), and cells were cultured for an additional 8 h at which point nuclear extracts were prepared. Biotinylated DNA probes derived from NFκB promoter DNA were either analyzed in the absence of cellular extracts (Ctrl: lanes 1, 4, and 7) or following incubation with untreated (mock: lanes 2, 5, and 8) or PU.1-transfected nuclear extracts (PU.1: lanes 3, 6, and 9). Samples were then processed as described in Fig. 4. Positions of probe and shifted samples are indicated on the right.

were separated by electrophoresis on a native 4.5% polyacrylamide gel, transferred to positively charged nylon membranes, and visualized by chemiluminescence using horseradish peroxidase (HRP)-conjugated streptavidin.

Using the pGL150 probes, we found a strong mobility shift for the wild-type probe in the presence of PU.1, which was efficiently competed by an unlabeled competitor probe (Fig. 4A, compare lanes 3 and 4). The probes containing mutated or deleted PU.1 boxes showed only marginal mobility shifts. The reduction in electrophoretic mobility was even more evident when the pGL135-based probes were analyzed (Fig. 4B). As with the pGL150-based samples, incubation of PU.1 with the wild-type probe produced a strong gel shift that was efficiently competed by the unlabeled competitor DNA (Fig. 4B, compare lanes 3 and 4). Importantly, mutation or deletion of the PU.1(b) box completely eliminated the PU.1-mediated gel shift (Fig. 4B, panels V and VI). These results identify the PU.1(b) element in the hMRC1 promoter as a direct binding site for PU.1 protein. The finding that deletion or mutation of the 5-bp PU.1(b) core sequence completely abolished PU.1 binding correlates well with the loss of PU.1 response in Fig. 3B [150-del(b) and 150-mut(b)]. Taken together, our results indicate that PU.1(b) represents a true binding site for PU.1 in the hMRC1 promoter.

To further demonstrate the specificity of the PU.1-mediated mobility shift of the hMRC1 promoter DNA fragment, we verified that the observed gel shifts are dose-dependent. For this, we prepared nuclear extracts containing increasing amounts of PU.1. This was accomplished by transfecting HEK293T cells separately with an empty vector (pcDNA3.1) or with pcDNA-PU.1-HA. Nuclear extracts were prepared 24 h after transfection, and extracts were mixed at various ratios as indicated in Fig. 5A. A fraction of the mixtures was subjected to immunoblot analysis using antibodies to the HA epitope on PU.1-HA or an SP1-specific antibody to demonstrate that all mixtures contained equivalent amounts of nuclear extracts (Fig. 5A, top). Mixtures #1 to #5 were then used for EMSA (Fig. 5B, EMSA) and immunoblot analysis (Fig. 5B, WBlot). As expected, the increased levels of PU.1 in the mixtures resulted in an increased shift of the biotinylated hMRC1 probe (Fig. 5B, EMSA, lanes 2–6). No gel shift was observed in the absence of nuclear extract (Fig. 5B, EMSA, lane 1), and the shift was competed by an excess unlabeled hMRC1 probe (Fig. 5B, EMSA, lane 7). Immunoblot analysis verified the presence of increasing amounts of PU.1 in the same area of the gel where the biotinylated hMRC1 probe migrated. It should be noted that the EMSA and WBlot analysis of samples in Fig. 5B were performed using 4.5% non-denaturing polyacrylamide gels. Thus, the pre-stained molecular weight standard shown on the right does not reflect the true size of PU.1-HA, which is predicted to be 31.5 kDa.

As a final specificity control, we assessed the impact of a mutation (S148A) located in the PEST domain of PU.1 on the ability to bind to the hMRC1 promoter DNA. It was previously reported that phosphorylation of PU.1 at a serine residue in the PEST domain (S148; see Fig. 7) was required for its interaction with NF-EM5 protein and recruitment to the immunoglobulin κ 3′ enhancer complex (24). In our own experiments, we did not observe a requirement of S148 phosphorylation for PU.1 activation of the hMRC1 promoter (2). To validate our results, we performed EMSA of PU.1 S148A in comparison with PU.1 wt. HEK293T cells were either mock transfected (Ctrl) or transfected with pcDNA-PU.1-HA wt or pcDNA-PU.1-HA S148A. Comparable PU.1 protein expression and equivalent nuclear extract (using nuclear SP1 as reference) were verified by immunoblotting (Fig. 5C). EMSA was performed as in Fig. 4. As expected, no gel shift occurred in the absence of PU.1 (Fig. 5D, lane 2). In contrast, efficient and comparable gel shift was observed in the presence of PU.1 wt (Fig. 5D, lane 3) or PU.1 S148A (Fig. 5D, lane 5). In both cases, the interaction of PU.1 with the hMRC1 probe was inhibited by the addition of excess unlabeled competitor DNA (Fig. 5D, lanes 4 and 6).

Transfer of the PU.1(b) binding motif to a heterologous promoter confers PU.1 responsiveness

Having identified PU.1(b) as a binding site for PU.1 on the hMRC1 promoter, we next studied whether the transfer of the PU.1(b) DNA element to a heterologous promoter could confer responsiveness to PU.1. We used pGL-3xNFκB as our test vector (25). This vector contains three NFκB binding sites in tandem upstream of a luciferase indicator

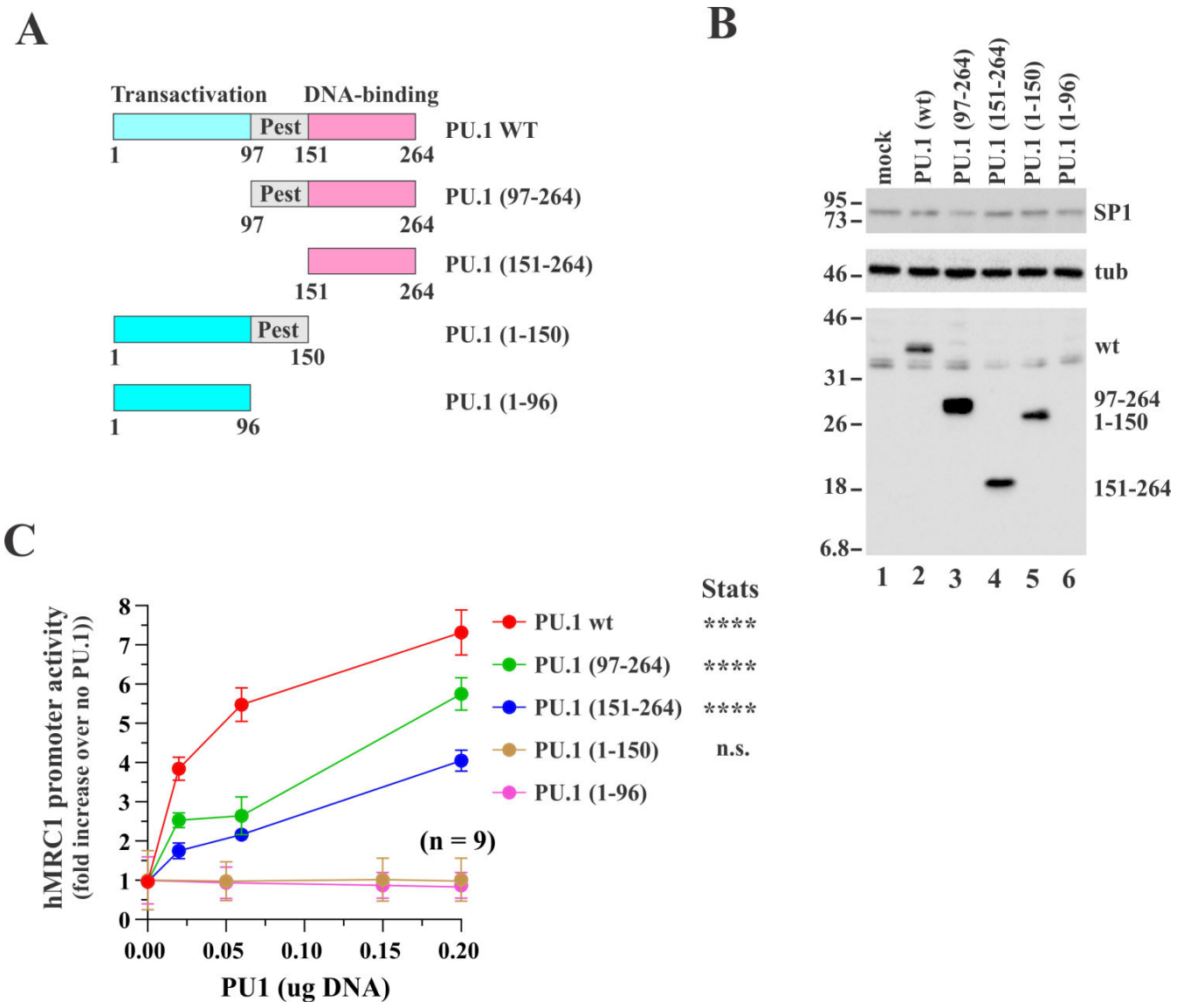

FIG 7 The DNA-binding domain in PU.1 is sufficient for binding to the hMRC1 promoter element. (A) Schematic representation of the constructs used in this analysis. N- and C-terminal deletions in PU.1 were constructed by oligonucleotide-based mutagenesis using pcDNA-PU.1-HA as a template together with the mutagenesis primers listed in Table 1. (B) Expression of truncated proteins was assessed by immunoblotting using an antibody to the HA epitope tag. Samples were also probed with antibodies to tubulin and SP1 for reference. (C) Activation of the hMRC1 promoter by PU.1 variants. HEK293T cells were transfected in 24-well plates with equal amounts (0.15 µg) of pGL150 indicator plasmid DNA together with increasing amounts of PU.1-HA(wt), PU.1 (97–264), PU.1 (151–264) (0, 0.02, 0.06, and 0.2 µg), or PU.1 (1–150) expression vector or empty vector (mock) (0. 0.05, 0.15, and 0.4 µg). Results were plotted as a function of PU.1 concentration. The luciferase activity observed in the absence of PU.1 was defined as 1. The effects of increasing amounts of PU.1 variants on hMRC1 promoter activation were expressed as fold change. All experiments were performed three times in triplicate (n = 9), and error bars represent the standard error of the mean. Statistical significance (Stats) of the differences of individual constructs at 0.2 µg PU.1 vectors relative to mock sample (mock) was determined using an unpaired two-tailed t-test (GraphPad Prism). n.s., not significant and ****P < 0.0001.

gene and has very low basal activity in HEK293T cells in the absence of NFκB stimulation. The nucleotide sequence of the promoter region in pGL-3xNFkB is shown in Fig. 6A. NFκB binding sites are indicated as blue boxes. A 15-bp sequence containing the PU.1(b) core sequence (TTCCT) plus five flanking nucleotides on each side (Fig. 6A, red sequence) was introduced independently at two different locations upstream of the NFκB sites on the pGL-3xNFκB-luc indicator plasmid. This was accomplished by oligonucleotide-based mutagenesis using the mutagenesis primers listed in Table 1.

When choosing the location for the insertion of the PU.1 boxes, we took advantage of the presence of two unique restriction enzyme cleavage sites in the pGL-3xNFκB promoter region for inserting the PU.1 boxes (Fig. 6A, BglII and PstI). The resulting vectors are schematically shown in Fig. 6B. Successful insertion of the PU.1(b) boxes led to the loss of either the BglII site (PU.1(b1) or the PstI site [PU.1(b2)] and was used as a tracer for discriminating between the various plasmid DNAs. PU.1 responsiveness of the resulting constructs was determined by transfecting constant amounts of the three indicator plasmids with increasing amounts of untagged wild-type PU.1 plasmid. Approximately 22 h post-transfection, cells were either treated with TNFα (Fig. 6C, solid circles) or left untreated (open circles) and luciferase production was determined 8 h later. In untreated cells, PU.1 expression did not cause an increase in luciferase activity with any of the indicator plasmids. Indeed, all signals remained at background levels. In contrast, treatment with TNFα resulted in the production of luciferase even in the absence of PU.1 (Fig. 6C, solid circles, 0 µg PU.1). As expected, the expression of PU.1 did not significantly increase luciferase expression in the absence of a PU.1 box (Fig. 6C, solid green circles). In contrast, the presence of a PU.1 box significantly increased luciferase activity (Fig. 6C, solid red and blue circles). There was a position dependence such that placing the PU.1 box closer to the NFκB sites slightly improved the PU.1 response. This positional effect was not statistically significant. The fact that PU.1 was unable to activate the PU.1 box containing vector in the absence of TNFα-induced NFκB could suggest that PU.1 alone is unable to assemble an active transcription complex, which is consistent with recent reports on the co-activator function of PU.1 (26, 27). EMSA confirmed that PU.1 was able to bind to the NFκB promoter probe if it contained a PU.1 box (Fig. 6D). Indeed, PU.1 seemed to bind more efficiently to the probe with a better PU.1 response in the luciferase assay when the PU.1 site was closer to the NFκB sites (Fig. 6C, compare solid blue to solid red graphs). Altogether, we conclude that the transfer of the PU.1(b) box to a heterologous promoter conferred responsiveness to the PU.1 transcriptional activator, thus validating the PU.1(b) box as a direct binding site for PU.1.

The C-terminal DNA-binding domain in PU.1 is critical for activating the hMRC1 promoter

Structural characterization of PU.1 revealed a three-domain organization (Fig. 7A). At the N-terminus is a transactivation domain that mediates the binding of PU.1 to various cellular factors. At the C-terminus is a DNA-binding domain that includes a nuclear localization signal as well as residues critical for the interaction with the PU.1 box (28). These domains are separated by a central PEST domain involved in stability, degradation, and protein-protein interactions (18, 21). Of note, a recent study reported the caspase 3-mediated cleavage of PU.1. The authors identified position D97 as a cleavage site of PU.1 giving rise to a 26-kDa protein. In addition, residue D151 was mapped as a less efficient cleavage site, producing a minor 15-kDa product (29). The functional relevance of the caspase-mediated cleavage of PU.1 remains unclear. We thus decided to characterize the functional properties of C- or N-terminally truncated PU.1 proteins. For that purpose, we constructed a series of PU.1 mutants as outlined in Fig. 7A. All constructs carry a C-terminal HA epitope tag to monitor their expression by immunoblotting using an HA-tag-specific antibody. Deletion of residues 2–96, which eliminates the entire transactivation domain, resulted in a 27-kDa protein that is identical to the 26-kDa caspase 3 cleavage product, except for the N-terminal methionine (defined here as residue 1). Of note, the resulting protein was expressed at higher levels than the full-length protein (Fig. 7B, compare lanes 2 and 3). Additional deletion of the PEST sequence (residues 2–150) from the N-terminus produced an 18-kDa protein that was expressed at levels comparable to the wild-type PU.1 (Fig. 7B, lane 4). Furthermore, eliminating the C-terminal DNA-binding domain produced a 26-kDa protein at near-wild-type levels (Fig. 7B, lane 5). PU.1 (1–96), lacking the PEST sequence as well as the C-terminal DNA-binding domain, did not express a stable protein and was therefore excluded from further analysis. We tested the ability of these PU.1 variants to

activate the hMRC1 promoter. For that purpose, HEK293T cells were transfected with constant amounts of pGL150 indicator plasmid DNA together with increasing amounts of PU.1(wt), N-terminal deletions PU.1 (97–264), and PU.1 (151–264), as well as the C-terminal truncation PU.1 (1–150). Activation of the hMRC1 promoter was assessed by luciferase assay as before. We found that deletion of the N-terminal transactivation domain modestly reduced the activation of the hMRC1 promoter (Fig. 7C, green line). Additional deletion of the PEST sequence from the N-terminus caused a further reduction in transcriptional activation but did not abolish PU.1 activity entirely (Fig. 7C, blue line). In contrast, deletion of the DNA-binding domain completely abolished the ability to activate the hMRC1 promoter (Fig. 7C, brown line) even though the protein was expressed at near wild-type levels. We conclude that the C-terminal DNA-binding domain in PU.1 is critical for the activation of the hMRC1 promoter, whereas the N-terminal transactivation domain plays a relatively minor role.

We wanted to ascertain that the ability to activate luciferase expression was correlated with the ability of the PU.1 variants to bind to the PU.1 box on the hMRC1 promoter. For that purpose, EMSA were performed (Fig. 8). HEK293T cells were transfected with HA-tagged PU.1 variants as described in Fig. 7B. Cytoplasmic (C) and nuclear (N) extracts were prepared as described in Materials and Methods. Successful fractionation was monitored by immunoblotting (Fig. 8A). We found that wild-type PU.1 as well as the N-terminal deletion mutants PU.1 (97–264) and PU.1 (151–264) partitioned between cytoplasmic and nuclear fractions. In contrast, deletion of the C-terminal DNA-binding domain restricted the expression of the PU.1 (1–150) variant to the cytoplasm. Consistent with this, EMSA, which employ nuclear extracts, confirmed the binding of wild-type and N-terminally deleted PU.1 proteins to the PU.1 box using the pGL150 probe employed in Fig. 4A (Fig. 8B, lanes 1–9). In contrast, PU.1 (1–150) lacking the C-terminal DNA-binding domain was unable to shift the EMSA probe (Fig. 8B, lanes 10–12). This was not surprising since this PU.1 variant was unable to enter the nucleus (Fig. 8A, lanes 9 and 10). Thus, we conclude that the N-terminal transactivation domain of PU.1 and the PEST sequence are not absolutely required for PU.1 binding to the PU.1(b) box on the hMRC1 promoter, but the DNA-binding domain is.

HIV-1 Tat interferes with the binding of PU.1 to the hMRC1 promoter

We previously showed that HIV-1 Tat interferes with the PU.1-dependent activation of the hMRC1 promoter (2). This function of Tat did not require transcriptional activity, but the underlying mechanism remained unclear. Initial attempts to demonstrate the interference of Tat with the binding of PU.1 to the hMRC1 promoter using EMSA of PU.1 in the presence of increasing amounts of transfected Tat vector were unsuccessful. We therefore resorted to the use of recombinant Tat protein. Tat protein (Tat 1–86) was expressed in *Escherichia coli* and purified as reported previously (30). The biological activity of the resulting protein was tested by titration on TZM-bl cells, which contain a Tat-responsive luciferase gene (Fig. 9A). Tat was prediluted in serum-free Dulbecco's modified Eagle's medium (DMEM) prior to addition to the cells. The highest concentration of recombinant Tat tested was 100 ng/mL (Fig. 9A, right column), followed by threefold serial dilution down to 1:243 (corresponding to 0.4 ng/mL). A sample lacking Tat was included as a control (left column). We observed a dose-dependent increase in Tat-induced luciferase activity that had not reached a plateau at the highest concentration of Tat tested.

We then tested the ability of Tat to interfere with the PU.1-mediated mobility shift of the hMRC1 promoter. The experiment was done essentially as described in Fig. 4A using the "150-wt" probe except that samples were treated for 30 min at room temperature with varying amounts of Tat protein as indicated above. In the absence of any cell extract, Tat did not cause a mobility shift indicating that Tat alone does not bind to the hMRC1 DNA probe (Fig. 9B, lanes 1–4). The addition of nuclear extract lacking PU.1 also did not cause a mobility shift of the hMRC1 probe (Fig. 9B, lanes 5–8), suggesting that even adding nuclear factors did not induce binding of Tat to the hMRC1 promoter DNA.

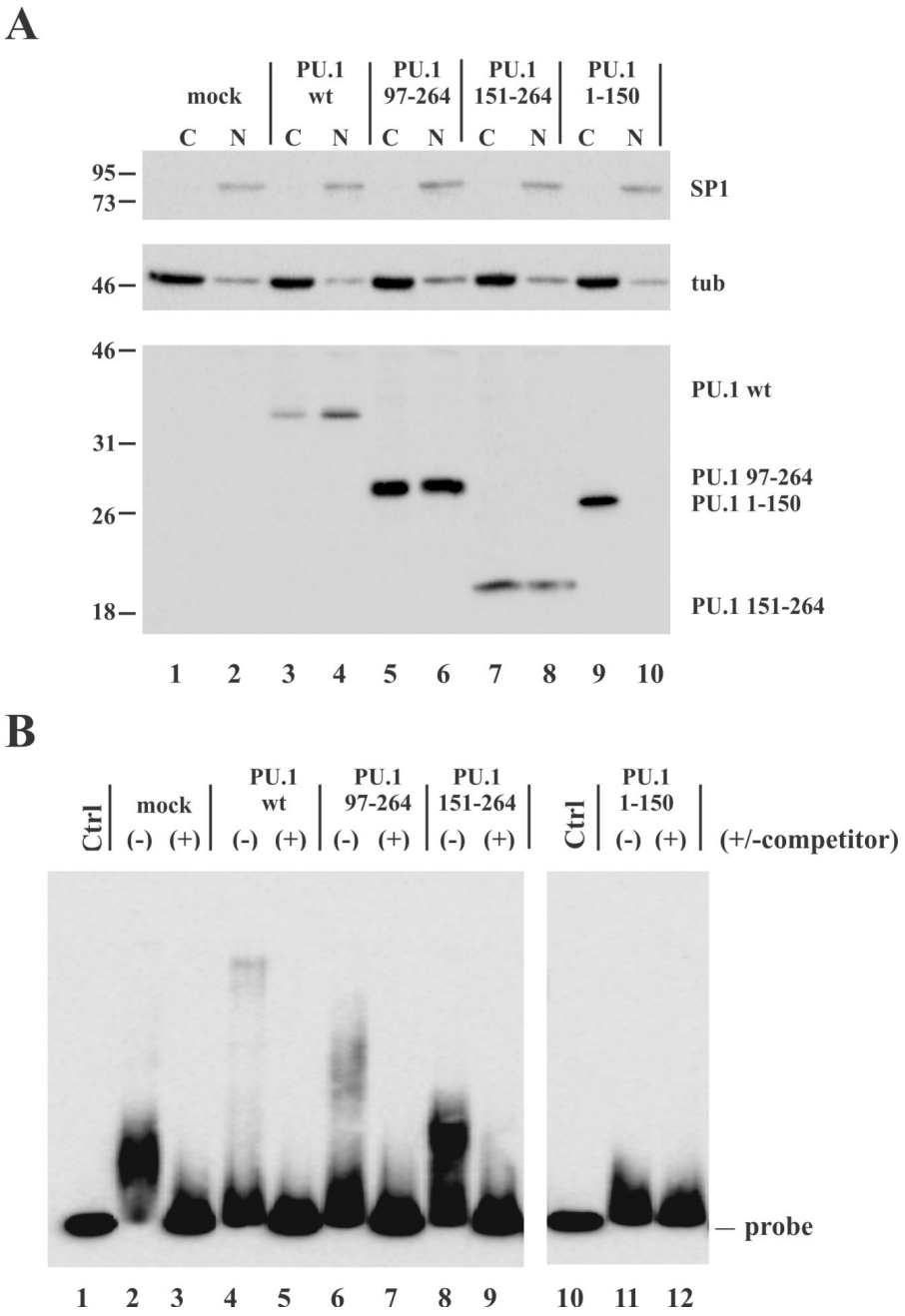

FIG 8 Activation of the hMRC1 promoter by PU.1 variants correlates with their ability to bind to the hMRC1 promoter region. (A) Subcellular localization of PU.1 variants. HEK293T cells were transfected with PU.1-HA and its deletion variants as shown at the top. Cytoplasmic and nuclear extracts were prepared using an NE-PER Nuclear and Cytoplasmic Extraction kit (Thermo Scientific, Rockport, IL, USA, Cat#78835) following the manufacturer's instructions. Extracts were subjected to SDS-13% PAGE and probed with an HA-specific antibody to visualize PU.1 (bottom). A parallel blot was probed with antibodies to tubulin (cytoplasmic marker) and SP1 (nuclear marker) (top). (B) EMSA of PU.1 variants. A biotinylated probe was produced as described in Fig. 4A. Nuclear extracts from panel A were incubated with a biotinylated probe and processed as described in Fig. 4A. All samples were analyzed on a single 8% native polyacrylamide gel. Irrelevant data between lanes 9 and 10 were cut off.

As expected, the addition of PU.1-containing nuclear extract induced a strong mobility shift in the absence of Tat (Fig. 9B, lane 9). Importantly, however, the addition of increasing amounts of recombinant Tat gradually reduced the gel shift signal (Fig. 9B, lanes 10–12). These results indicate that Tat interferes with the PU.1-mediated activation of the

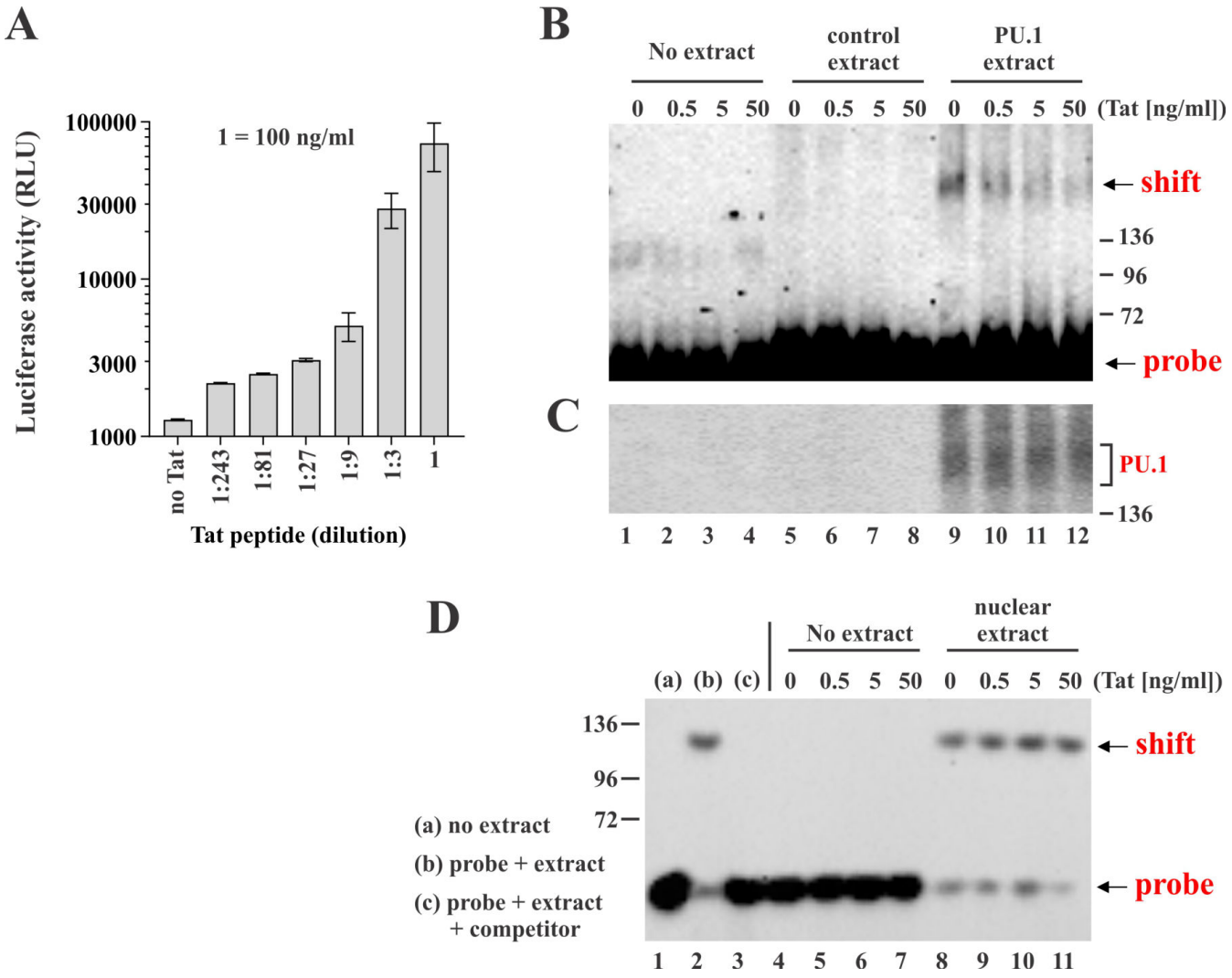

FIG 9 HIV-1 Tat interferes with the PU.1-dependent mobility shift of the hMRC1 promoter. (A) Recombinant Tat protein activity was assessed by using the Tat-dependent activation of the luciferase gene in TZMbl cells as readout. Tat protein was diluted in serum-free medium to 100 ng/mL, followed by additional threefold serial dilutions; 500 µL of each dilution was added to three wells each of TZMbl cells in a 24-well plate. Tat's buffer was used as a control. After 5 h, 500 µL of DMEM containing 20% fetal bovine serum (FBS) were added to each well, and samples were incubated overnight. Luciferase activity was then determined in a standard luciferase assay. Error bars show the standard error of the mean, calculated from the three replicate samples. (B) EMSA reveals interference of recombinant Tat with PU.1-mediated gel shift of the hMRC1 promoter. The experiment was similarly performed as described in Fig. 4A using the "150-wt" probe except that samples were treated for 30 min at room temperature with varying amounts of Tat protein as indicated above. Lanes 1–4: probe only; lanes 5–8: control nuclear extract without PU.1; and lanes 9–12: nuclear extract containing PU.1. Concentration of Tat protein in each lane is indicated at the top. Positions of unshifted probe (probe) and shifted probe (shift) are indicated on the right. A representative of four independent experiments is shown. (C) The presence of equal amounts of PU.1 in lanes 9–12 was verified by immunoblotting as described in Fig. 5B. The position of PU.1 is indicated on the right. (D) Specificity control for the interference of PU.1-mediated gel shift of the hMRC1 promoter by Tat. We used a control provided by the manufacturer of the EMSA kit. Biotin-labeled 60-bp duplex bearing the Epstein-Barr nuclear antigen (EBNA-1) binding sequence was incubated with an extract in which the EBNA-1 protein was overexpressed. Tat protein was added as in panel B and the gel shift analysis was done as in panel B. (a) Biotinylated EBNA probe without extract; (b) biotinylated EBNA probe with EBNA-containing nuclear extract; (c) biotinylated EBNA probe containing nuclear extract and 100-fold excess of unlabeled EBNA probe. Lanes 4–7: biotinylated EBNA probe without nuclear extract containing increasing amounts of Tat protein; lanes 8–11: biotinylated EBNA probe containing nuclear extract and increasing amounts of Tat protein. A representative of three independent experiments is shown.

hMRC1 promoter by interfering with PU.1 binding to the hMRC1 promoter element. The presence of equal amounts of PU.1 in the shifted complex was verified by immunoblotting as described in Fig. 5B. This control demonstrates that recombinant Tat did not

cause degradation or otherwise depletion of PU.1 available for binding to the hMRC1 promoter DNA (Fig. 9C).

To rule out the possibility that the inhibition of the PU.1 gel shift by Tat in panel B (Fig. 9B) is a technical artifact, we tested the effect of recombinant Tat on the gel shift of an unrelated probe. We took advantage of the fact that the EMSA kit used for our assays included as a positive control the Epstein-Barr nuclear antigen (EBNA) System, which consists of a biotinylated EBNA DNA probe and EBNA protein extract (Fig. 9D). An initial control shows the position of the biotinylated probe in the absence of nuclear extract and Tat (Fig. 9D, lane 1). The shift of the EBNA DNA probe after the addition of EBNA protein-containing extract is shown in lane 2, and the competition of the EBNA gel shift in the presence of a 100-fold excess of unlabeled EBNA DNA probe is shown in lane 3. The addition of Tat to the biotinylated probe in the absence of EBNA protein-containing extract did not result in a gel shift, confirming that recombinant Tat protein alone does not bind to the EBNA promoter DNA (Fig. 9D, lanes 4–7). As expected, combining the EBNA protein-containing nuclear extract with the biotinylated EBNA DNA probe induced a solid gel shift in the absence of Tat (Fig. 9D, lane 8). Importantly, the addition of increasing amounts of Tat did not interfere with the formation of complexes of EBNA protein and EBNA DNA. These results demonstrate that the interference of Tat with PU.1 binding to the hMRC1 promoter is indeed specific.

DISCUSSION

The experiments reported here were done as a follow-up to a previous study in which we reported that HIV-1 Tat inhibits hMRC1 expression in HIV-1-infected human macrophages by interfering with the PU.1-dependent regulation of its promoter (2). The premise for the current study was to obtain a detailed understanding of the regulation of the hMRC1 promoter by PU.1 as basis for understanding the role of Tat in the process of hMRC1 silencing. It is well known that transcriptional regulation of mammalian genes is highly complex and involves the binding of defined transcription factors to specific DNA elements known as enhancers [for review see reference (31)]. Enhancers are DNA elements that are typically located near the transcription start site but can also be located at various distances upstream or downstream from the transcription start site and are generally orientation independent (32). In the case of the hMRC1 promoter, we identified four potential PU.1 boxes with the core motif 5′-TTCCT-3′ (Fig. 1). Interestingly, only one of the four potential PU.1 binding sites, PU.1(b), was used by PU.1 suggesting that the actual PU.1 binding site on the promoter is defined by more than the five base pair core motif. It is likely that flanking sequences may be important as well. This is the reason we chose to transfer the PU.1(b) core element together with a 5-bp flanking sequence on each side into the heterologous NFκB-dependent test vector described in Fig. 6. It is interesting that in this active PU.1 box, the pyrimidine-based TTCCT motif is flanked by purine residues on either side, a feature that is not conserved in the other three PU.1 boxes. The contribution of flanking sequences to the function of a PU.1 box may also explain a seeming discrepancy between results from Fig. 2 and 3. In Fig. 2, we observed that the elimination of PU.1(a) together with all upstream promoter sequences (i.e., pGL135 and pGL90) resulted in an approximately 50% loss of PU.1 responsiveness, implying that PU.1(a) and PU.1(b) equally contribute to PU.1 responsiveness. In contrast, the more subtle changes made in Fig. 3, rendered the PU.1(b) mutants largely insensitive to PU.1 [Fig. 3B, 150-del(b) and 150-mut(b)], while mutation or deletion of the PU.1(a) had basically no effect on PU.1 responsiveness [Fig. 3B, 150-del(a) and 150-mut(a)]. We therefore conclude that the PU.1(b) box is the primary binding site for PU.1 in the context of the full promoter, and its surrounding nucleotides may contribute to PU.1 binding.

Our analysis of PU.1 truncations (Fig. 7) revealed that expression of the C-terminal region of PU.1 that includes the DNA-binding domain is sufficient to retain at least partially the ability to activate the hMRC1 promoter. This is consistent with a previous report that found that PU.1 could participate in the assembly of active enhancer complexes without its transcriptional activation domain (33). Results from that study

show that binding of PU.1 to its target DNA can recruit secondary transcription factors that promote transcriptional activation. In those contexts, PU.1 appears to play an architectural role in the assembly of higher-order protein-DNA complexes (33). It was also previously reported that phosphorylation of PU.1 at a serine residue in the PEST domain (S148) was required for its interaction with NF-EM5 and recruitment to the immunoglobulin κ 3′ enhancer complex (24). We previously analyzed an S148A mutant of PU.1 and found that it activated the hMRC1 promoter with similar efficiency to the wild-type protein (2). In line with this result, the N-terminal deletion mutant, PU.1 (151–264), lacking the entire PEST domain, still retained about 50% activity compared to the wild-type protein (see Fig. 7C). EMSA performed here using PU.1 wt and PU.1 S148A further confirmed that, at least in HEK293T cells, phosphorylation of PU.1 is not critically important for PU.1 binding to its DNA element (Fig. 5D).

Our study does not directly address the question of how the HIV-1 Tat protein inhibits the PU.1-mediated activation of the hMRC1 promoter as previously reported (1, 2). Unlike PU.1, which binds to a specific DNA element (the PU.1 box) on the hMRC1 promoter, Tat binds to the HIV-1 TAR element on the viral RNA but has not been reported to function as a DNA-binding protein. Here, we found that Tat alone did not bind the hMRC1 promoter element in an EMSA (Fig. 9). Interestingly, however, Tat interfered in a dose-dependent manner with the binding of PU.1 to the hMRC1 promoter element. Attempts to demonstrate the interaction of Tat and PU.1 by co-immunoprecipitation were so far unsuccessful. It seems therefore unlikely that Tat inhibits PU.1 through the formation of transcriptionally inactive hetero oligomeric PU.1-Tat complexes. Since PU.1 is involved in the recruitment of multiple other transcription factors [for review see reference (18)], it is conceivable that Tat competitively interferes with the formation of PU.1-based transcription complexes involving other transcriptional (co)factors.

MATERIALS AND METHODS

Cells

HEK293T cells were maintained in Dulbecco's modified Eagle's medium with 4.5 g/L glucose (Sigma-Aldrich, St. Louis, MO, USA), supplemented with 10% fetal bovine serum, 100 U/mL penicillin, and 100 µg/mL streptomycin in a 37°C and 5.0% CO_2 environment.

Plasmids and viral vectors

A PU.1 (SPI1) cDNA (GenBank BC111379) clone was purchased from Dharmacon (Catalog ID: OHS5898-202627596) and cloned in untagged form into pcDNA3.1(–) as reported (2). For the analysis of PU.1 truncation mutants (Fig. 7), a C-terminal HA-tag (YPYDVPDYA) was added via oligonucleotide-based mutagenesis using oligonucleotide primers listed in Table 1. Wild-type pcDNA-PU.1 served as a PCR template. The HA-tag is encoded by the 3′ PCR primer. The resulting PCR products were digested with XhoI and BamHI and cloned into the corresponding sites of pcDNA-PU.1. The proper in-frame addition of the HA-tag was confirmed by sequence analysis.

The mannose receptor promoter vector pGL284 was constructed as follows: based on the hMRC1 promoter sequence reported by Rouleux et al. (23) and cross comparison with GenBank entry NG_047011.1 (positions 4,703–5,021), a 342-bp gBlock DNA fragment was synthesized (IDT, Coralville, IA, USA). The gBlock fragment encompassed residues −284 to +36 of the *hMRC1* gene. In addition, an upstream HindIII site and a downstream NcoI restriction site were added to the gBlock sequence and used for cloning into the promoter trap vector pGL3-basic (Promega, Madison, WI, USA), which contains a luciferase gene downstream of a multicloning site. Consequently, the transcriptional activity of promoter elements cloned into pGL3-basic upstream of the luciferase gene was determined using a standard luciferase assay. Variants of pGL284 were constructed by oligonucleotide-based mutagenesis using the primer pairs listed in Table 1. The pGL150 vector was described recently (2). All other hMRC1-Luc vectors

were created by PCR-based mutagenesis using the primer pairs listed in Table 1. Plasmid pGL-3xNFκB carrying three NFκB sites upstream of a luciferase indicator gene was a gift of Venkat Yedavalli.

Oligonucleotide-based mutagenesis

Insertions, deletions, or nucleotide changes were created using pairs of complementary synthetic oligonucleotide primers as listed in Table 1. Typically, oligonucleotides were designed to include the desired mutations, deletions, or insertions flanked by 16 nucleotides of matching sequences. Mutagenesis was performed using PfuUltra HF DNA polymerase (Agilent, Santa Clara, CA, USA). Typical reactions consisted of 10 ng template DNA, 13 pmol each of forward and reverse primers containing the desired changes, 200 µM dNTPs, 1× Pfu reaction buffer, and 2.5 U PfuUltra HF in a 50 µL reaction volume. Samples were overlaid with one drop of mineral oil to prevent sample evaporation during the PCR amplification. Typical PCR amplification conditions were initial denaturation of 5 min at 95°C, followed by 16 cycles of 45 s at 95°C, 1.5 min at 45°C, and 6 min at 68°C (1 min + 1 additional minute per 1-kb template DNA). This was followed by a final 10-min incubation at 68°C to allow the DNA polymerase to fill any remaining gaps in the DNA. After completion of the PCR amplification, samples were transferred to a fresh tube to eliminate most of the mineral oil. Samples were then incubated for 60 min with 10 U DpnI restriction enzyme to digest the methylated template DNA. The *in vitro*-synthesized mutated DNA is unmethylated and therefore resistant to DpnI digestion. After the DpnI digest, 10%–20% of the sample was used to transform competent *E. coli* JM109. Individual colonies were picked, and the successful mutagenesis was verified by sequence analysis.

Transient transfection of HEK293T cells for immunoblot analyses

For transient transfection of HEK293T cells, 3×10^6 cells were plated in a 25-cm^2 flask and grown overnight. The following day, cells were transfected using Lipofectamine PLUS (Invitrogen Corp, Carlsbad, CA, USA) according to the manufacturer's instructions. Total amounts of plasmid DNAs in all samples were adjusted to 5 µg with empty vector DNA as appropriate. After 24 h, whole cell extracts were produced as follows: cells were scraped, washed with PBS, suspended in PBS (100 µL/10^6 cells), and mixed with an equal volume of 2× sample buffer [4% SDS, 125 mM Tris-HCl (pH 6.8), 10% 2-mercaptoethanol, 10% glycerol, and 0.002% bromophenol blue]. Samples were heated for 10–15 min at 95°C with occasional vortexing to shear cellular DNA. Samples were then processed for immunoblot analysis.

Transient transfection of HEK293T cells for luciferase assays

For transient transfection of HEK293T cells, cells were plated into 24-well plates (1×10^5 cells per well in 1 mL). The following day, cells were transfected using Lipofectamine PLUS (Invitrogen Corp, Carlsbad, CA, USA) as follows: the medium was removed from 24-well plates and replaced by 0.5 mL of serum-free DMEM. DNA samples (typically 2.5 µg total DNA; see figure legends) were mixed with 150 µL of serum-free DMEM containing 6 µL of Plus reagent. After 15 min, 150 µL of serum-free DMEM containing 6.5 µL of Lipofectamine reagent was added to the DNA-containing samples for a total volume of 325 µL. After 15-min incubation at room temperature, 50 µL of transfection mix was added to each of the three wells. The remaining transfection mix was discarded. After 24 h, the medium was aspirated from plates, 250 µL of 1× Promega lysis buffer (Promega, Cat# E397A) was added, and the plates were transferred to a −80°C freezer for at least 30 min. Then, the plates were warmed to 37°C for 30 min, and 15 µL of lysate from each well was mixed with 50 µL of Steady Glo substrate (Promega, Cat# E2510). After 5-min incubation at room temperature, light emission was measured in a Promega GloMax Explorer.

Immunoblot analysis

Cells were washed once with PBS, suspended in PBS (100 µL/10^6 cells), and mixed with an equal volume of 2× sample buffer. Samples were heated at 95°C with occasional vortexing until samples were completely dissolved. Samples (20–30 µL) were subjected to SDS-PAGE, transferred to polyvinylidene difluoride membranes, and reacted with primary antibodies as described earlier. To enhance sensitivity, SignalBoost Immunoreaction Enhancer Kit (CalBiochem, Cat# 407207-1KIT) was employed in some of the experiments. Tubulin was identified using a mouse monoclonal antibody to alpha-tubulin (Cat#T9026, Sigma-Aldrich Inc., St. Louis, MO, USA), and the nuclear marker Sp1 was identified using a rabbit monoclonal antibody (Cat#sc-59, Santa Cruz Biotechnology Inc., Dallas, TX, USA). Flag-tagged PU.1 was identified using an HRP-conjugated anti-Flag monoclonal antibody (Cat# A8592, Sigma-Aldrich Inc., St. Louis, MO, USA). The rabbit monoclonal antibody to PU.1 was from Abcam (Cat# ab76543, Abcam, Boston, MA, USA). The membranes were then incubated with horseradish peroxidase-conjugated secondary antibodies (GE Healthcare, Piscataway, NJ, USA), and proteins were visualized by enhanced chemiluminescence (ClarityTM Western ECL substrate #170-5061, Bio-Rad Laboratories, Hercules, CA, USA).

Electrophoretic mobility shift assay

DNA probes for the EMSA of hMRC1 or NFκB promoter elements were produced by PCR amplification using primer pairs listed in Table 1 and templates as indicated in the figure legends. PCR products were purified using a QIAquick PCR purification kit (Qiagen, Cat#28104). A Thermo Scientific Pierce Biotin 3′ End DNA Labeling Kit (Thermo Fisher Scientific, Cat # 89818) was then used to biotinylate the purified DNA probes. For the expression of wt PU.1 and PU.1 variants, HEK293T cells were mock transfected or transfected with PU.1 expression vectors as indicated in the text. Nuclear extracts were prepared 24 h later using a NE-PER Nuclear and Cytoplasmic Reagent Extraction Kit (Thermo Fisher, Cat#78835). For mobility shift assays, nuclear extracts were incubated with biotinylated DNA probes using a LightShift Chemiluminescent EMSA Kit (Thermo Scientific, Cat#20148). Binding of the probe to nuclear extracts, gel electrophoresis, transfer at 380 mA to the positively charged nylon membrane, UV crosslinking, and chemiluminescence were done following the manufacturer's instructions. The specificity of the gel shift was verified in a competition reaction containing excess (>100×) amounts of unlabeled probes together with the biotinylated probe.

Bacterial expression and purification of recombinant Tat

pTatC6H-1 plasmid (NIH HIV Reagent Program, Cat # ARP-3423) encoding C-terminal 6xHistidine Tat1-86 (HXB3, subtype B) was expressed in *E. coli* BL 21 to obtain Tat protein. Recombinant Tat protein was induced with isopropyl β-D-thio-galactopyranoside and purified as described in the AIDS Reagent Program procedure. The active monomeric form of Tat was then obtained upon filtration with a 30-kDa filter (Millipore) and solubilization in acidic phosphate buffer (pH ≈ 4) to prevent cysteine residue oxidation (30). The mass and purity of the Tat protein were subsequently verified by SDS-PAGE and western blot. The transactivation activity of the recombinant Tat was verified in a transactivation assay. Briefly, HeLa-CD4-LTR-Luc cells were plated at 1×10^5 cells per well in a 6-well plate. The following day, recombinant Tat protein was added to the cells without serum and in the presence of 100 µM of chloroquine. Four hours later, serum was added at 5% to the media. Cells were lysed 24 h later. Protein concentration was determined by Bradford assay (BioRad protein assay), and luciferase activity was measured with the luciferase assay system (Promega).

Statistical analysis

The average values of all the data are presented with error bars indicating the standard error of the median. Statistical significance was determined using GraphPad Prism as indicated in the figure legends.

ACKNOWLEDGMENTS

The following reagents were obtained through the NIH HIV Reagent Program, Division of AIDS, NIAID, NIH: HIV-1 immunoglobulin (Cat #3957), contributed by NABI and National Heart Lung and Blood Institute (Dr. Luiz Barbosa). TZM-bl indicator cells (Cat# ARP-8129) were contributed by Dr. John C. Kappes, Dr. Xiaoyun Wu, and Tranzyme Inc. Plasmid pTatC6H-1 (NIH AIDS Reagent Program, Cat # ARP-3423).

This work was supported by the Intramural Research Program of the NIH, NIAID (1 Z01 AI000669; K.S.). Extramural support was provided to S.V.: R21 AI158296, R01 AI097012, and R01DA052027.

AUTHOR AFFILIATIONS

[1]Viral Biochemistry Section, Laboratory of Molecular Microbiology, NIAID, NIH, Bethesda, Maryland, USA
[2]Department of Molecular Virology, Graduate School of Medical and Dental Sciences, Tokyo Medical and Dental University (TMDU), Tokyo, Japan
[3]Department of Immunology and Microbiology, The Herbert Wertheim UF Scripps Institute for Biomedical Innovation and Technology, Jupiter, Florida, USA

AUTHOR ORCIDs

Rosa Mallorson http://orcid.org/0000-0002-1644-0321
Eri Miyagi http://orcid.org/0000-0001-9561-2269
Susana T. Valente http://orcid.org/0000-0002-7854-7554
Klaus Strebel http://orcid.org/0000-0002-2827-8923

FUNDING

Funder	Grant(s)	Author(s)
HHS | NIH | NIAID | Division of Intramural Research, National Institute of Allergy and Infectious Diseases (DIR, NIAID)	1 Z01 AI000669	Klaus Strebel
HHS | NIH | National Institute of Allergy and Infectious Diseases (NIAID)	AI158296	Susana T. Valente
HHS | NIH | National Institute of Allergy and Infectious Diseases (NIAID)	AI097012	Susana T. Valente
HHS | NIH | National Institute of Allergy and Infectious Diseases (NIAID)	DA052027	Susana T. Valente

AUTHOR CONTRIBUTIONS

Rosa Mallorson, Data curation, Investigation, Validation | Eri Miyagi, Conceptualization, Data curation, Formal analysis, Supervision | Sandra Kao, Data curation, Investigation | Sayaka Sukegawa, Formal analysis, Investigation | Hideki Saito, Data curation, Investigation | Helena Fabryova, Investigation, Methodology | Luciana Morellatto Ruggieri, Data curation, Formal analysis | Sonia Mediouni, Methodology | Susana T. Valente, Methodology | Klaus Strebel, Conceptualization, Funding acquisition, Project administration, Supervision, Writing – review and editing

REFERENCES

1. Sukegawa S, Miyagi E, Bouamr F, Farkašová H, Strebel K. 2018. Mannose receptor 1 restricts HIV particle release from infected macrophages. Cell Rep 22:786–795. https://doi.org/10.1016/j.celrep.2017.12.085
2. Kao S, Miyagi E, Mallorson R, Saito H, Sukegawa S, Mukherji A, Mateja A, Ferhadian D, Fabryova H, Clouse K, Strebel K. 2022. The myeloid-specific transcription factor PU.1 upregulates mannose receptor expression but represses basal activity of the HIV-LTR promoter. J Virol 96:e0065222. https://doi.org/10.1128/jvi.00652-22
3. Andrew A, Strebel K. 2011. The interferon-inducible host factor bone marrow stromal antigen 2/tetherin restricts virion release, but is it actually a viral restriction factor? J Interferon Cytokine Res 31:137–144. https://doi.org/10.1089/jir.2010.0108
4. Caldwell RL, Egan BS, Shepherd VL. 2000. HIV-1 Tat represses transcription from the mannose receptor promoter. J Immunol 165:7035–7041. https://doi.org/10.4049/jimmunol.165.12.7035
5. Lubow J, Virgilio MC, Merlino M, Collins DR, Mashiba M, Peterson BG, Lukic Z, Painter MM, Gomez-Rivera F, Terry V, Zimmerman G, Collins KL. 2020. Mannose receptor is an HIV restriction factor counteracted by Vpr in macrophages. Elife 9:e51035. https://doi.org/10.7554/eLife.51035
6. Vigerust DJ, Egan BS, Shepherd VL. 2005. HIV-1 nef mediates post-translational down-regulation and redistribution of the mannose receptor. J Leukoc Biol 77:522–534. https://doi.org/10.1189/jlb.0804454
7. Jeang KT. 1998. Tat, Tat-associated kinase, and transcription. J Biomed Sci 5:24–27. https://doi.org/10.1007/BF02253352
8. Jones KA. 1997. Taking a new TAK on Tat transactivation. Genes Dev 11:2593–2599. https://doi.org/10.1101/gad.11.20.2593
9. Clark E, Nava B, Caputi M. 2017. Tat is a multifunctional viral protein that modulates cellular gene expression and functions. Oncotarget 8:27569–27581. https://doi.org/10.18632/oncotarget.15174
10. Rice AP. 2017. The HIV-1 Tat protein: mechanism of action and target for HIV-1 cure strategies. Curr Pharm Des 23:4098–4102. https://doi.org/10.2174/1381612823666170704130635
11. Barboric M, Fujinaga K. 2016. The two sides of Tat. Elife 5:e12686. https://doi.org/10.7554/eLife.12686
12. Reeder JE, Kwak Y-T, McNamara RP, Forst CV, D'Orso I. 2015. HIV Tat controls RNA polymerase II and the epigenetic landscape to transcriptionally reprogram target immune cells. Elife 4:e08955. https://doi.org/10.7554/eLife.08955
13. Ray D, Culine S, Tavitain A, Moreau-Gachelin F. 1990. The human homologue of the putative proto-oncogene Spi-1: characterization and expression in tumors. Oncogene 5:663–668.
14. Turkistany SA, DeKoter RP. 2011. The transcription factor PU.1 is a critical regulator of cellular communication in the immune system. Arch Immunol Ther Exp (Warsz) 59:431–440. https://doi.org/10.1007/s00005-011-0147-9
15. De Smedt J, van Os EA, Talon I, Ghosh S, Toprakhisar B, Furtado Madeiro Da Costa R, Zaunz S, Vazquez MA, Boon R, Baatsen P, Smout A, Verhulst S, van Grunsven LA, Verfaillie CM. 2021. PU.1 drives specification of pluripotent stem cell-derived endothelial cells to LSEC-like cells. Cell Death Dis 12:84. https://doi.org/10.1038/s41419-020-03356-2
16. Fisher RC, Scott EW. 1998. Role of PU.1 in hematopoiesis. Stem Cells 16:25–37. https://doi.org/10.1002/stem.160025
17. Imperato MR, Cauchy P, Obier N, Bonifer C. 2015. The RUNX1-PU.1 axis in the control of hematopoiesis. Int J Hematol 101:319–329. https://doi.org/10.1007/s12185-015-1762-8
18. Gupta P, Gurudutta GU, Saluja D, Tripathi RP. 2009. PU.1 and partners: regulation of haematopoietic stem cell fate in normal and malignant haematopoiesis. J Cell Mol Med 13:4349–4363. https://doi.org/10.1111/j.1582-4934.2009.00757.x
19. Egan BS, Lane KB, Shepherd VL. 1999. PU.1 and USF are required for macrophage-specific mannose receptor promoter activity. J Biol Chem 274:9098–9107. https://doi.org/10.1074/jbc.274.13.9098
20. Klemsz MJ, McKercher SR, Celada A, Van Beveren C, Maki RA. 1990. The macrophage and B cell-specific transcription factor PU.1 is related to the ets oncogene. Cell 61:113–124. https://doi.org/10.1016/0092-8674(90)90219-5
21. Celada A, Borràs FE, Soler C, Lloberas J, Klemsz M, van Beveren C, McKercher S, Maki RA. 1996. The transcription factor PU.1 is involved in macrophage proliferation. J Exp Med 184:61–69. https://doi.org/10.1084/jem.184.1.61
22. Zhang DE, Hetherington CJ, Chen HM, Tenen DG. 1994. The macrophage transcription factor PU.1 directs tissue-specific expression of the macrophage colony-stimulating factor receptor. Mol Cell Biol 14:373–381. https://doi.org/10.1128/mcb.14.1.373-381.1994
23. Rouleux F, Monsigny M, Legrand A. 1994. A negative regulatory element of the macrophage-specific human mannose receptor gene represses its expression in nonmyeloid cells. Exp Cell Res 214:113–119. https://doi.org/10.1006/excr.1994.1239
24. Pongubala JM, Van Beveren C, Nagulapalli S, Klemsz MJ, McKercher SR, Maki RA, Atchison ML. 1993. Effect of PU.1 phosphorylation on interaction with NF-EM5 and transcriptional activation. Science 259:1622–1625. https://doi.org/10.1126/science.8456286
25. Mitchell T, Sugden B. 1995. Stimulation of NF-kappa B-mediated transcription by mutant derivatives of the latent membrane protein of Epstein-Barr virus. J Virol 69:2968–2976. https://doi.org/10.1128/JVI.69.5.2968-2976.1995
26. Nagulapalli S, Pongubala JM, Atchison ML. 1995. Multiple proteins physically interact with PU.1. Transcriptional synergy with NF-IL6 beta (C/EBP delta, CRP3). J Immunol 155:4330–4338.
27. Hohaus S, Petrovick MS, Voso MT, Sun Z, Zhang DE, Tenen DG. 1995. PU.1 (Spi-1) and C/EBP alpha regulate expression of the granulocyte-macrophage colony-stimulating factor receptor alpha gene. Mol Cell Biol 15:5830–5845. https://doi.org/10.1128/MCB.15.10.5830
28. Kwok JC, Perdomo J, Chong BH. 2007. Identification of a monopartite sequence in PU.1 essential for nuclear import, DNA-binding and transcription of myeloid-specific genes. J Cell Biochem 101:1456–1474. https://doi.org/10.1002/jcb.21264
29. Zhao M, Duan X-F, Wen D-H, Chen G-Q. 2009. PU.1, a novel caspase-3 substrate, partially contributes to chemotherapeutic agents-induced apoptosis in leukemic cells. Biochem Biophys Res Commun 382:508–513. https://doi.org/10.1016/j.bbrc.2009.03.024
30. Mediouni S, Jablonski J, Paris JJ, Clementz MA, Thenin-Houssier S, McLaughlin JP, Valente ST. 2015. Didehydro-cortistatin A inhibits HIV-1 Tat mediated neuroinflammation and prevents potentiation of cocaine reward in Tat transgenic mice. Curr HIV Res 13:64–79. https://doi.org/10.2174/1570162x13666150121111548
31. Wilkinson AC, Nakauchi H, Göttgens B. 2017. Mammalian transcription factor networks: recent advances in interrogating biological complexity. Cell Syst 5:319–331. https://doi.org/10.1016/j.cels.2017.07.004
32. Pennacchio LA, Bickmore W, Dean A, Nobrega MA, Bejerano G. 2013. Enhancers: five essential questions. Nat Rev Genet 14:288–295. https://doi.org/10.1038/nrg3458
33. Pongubala JM, Atchison ML. 1997. PU.1 can participate in an active enhancer complex without its transcriptional activation domain. Proc Natl Acad Sci U S A 94:127–132. https://doi.org/10.1073/pnas.94.1.127